Photoproduction of light η nuclei

V. A. Tryasuchev
Tomsk Polytechnic University

Fiz. Élem. Chastits At. Yadra **30**, 1391–1428 (November–December 1999)

The hypothetical existence of η nuclei, including superlight ones ($A=3$), is discussed in the light of the new data and the nuclear model with an optical potential. The quasifree photoproduction of η mesons on light nuclei is used as the basis for constructing a systematic model of η-nucleus photoproduction in reactions $\gamma+A\to N+{}_{\eta}A'$. The dependence of the cross sections for such reactions on the main proposed properties of η nuclei is discussed, along with the final-state interaction for incident γ energies in the range from threshold to 1 GeV. © *1999 American Institute of Physics.* [S1063-7796(99)00206-5]

INTRODUCTION

In the symmetric three-quark model of hadrons, the two orthogonal superpositions of the lowest quark–antiquark states

$$\eta_8=\frac{1}{\sqrt{6}}(u\bar{u}+d\bar{d}-2s\bar{s}),$$

$$\eta_1=\frac{1}{\sqrt{3}}(u\bar{u}+d\bar{d}+s\bar{s}), \tag{1}$$

respectively pertaining to the octet and the singlet of pseudoscalar mesons, are degenerate states, and the wave functions of the η and η' mesons are a coherent mixture of the states (1):

$$\eta=\eta_8\cos\theta_p-\eta_1\sin\theta_p,$$

$$\eta'=\eta_8\sin\theta_p-\eta_1\cos\theta_p \tag{2}$$

with mixing angle θ_p. The approximate nature of the hadron $SU(3)$ symmetry is manifested in the different masses of the observed mesons $\eta(547)$ and $\eta'(958)$, and the absolute value of θ_p is determined from the Gell–Mann–Okubo mass formula. Although the quark content of the η mesons is not exhausted by the u, d, and s flavors, the contributions of heavier quarks can be neglected in what follows. The η meson in which we are interested, with mass 547.45 MeV/c^2 and lifetime 5.5×10^{-19} sec (Ref. 1), differs from the well studied π^0 meson not only in mass, but also in isospin. It is therefore interesting to make a comparative analysis of the interaction of baryons with π mesons and η mesons in order to test the main ideas of the theory of strong interactions, in particular, the isospin conservation law. The low-energy S-wave πN interaction is characterized by repulsion in the state with isospin 1/2 and a small attraction in the state with isospin 3/2, and the πN scattering length is close to 0 and of indefinite sign,[2] while the interaction of an η meson with a nucleon at low energies is characterized by a sizable attraction. This formed the basis of the hypothesis that η-meson–nucleus bound states, called η nuclei, exist.[3,4] The proof of the existence of η nuclei is an important problem in intermediate-energy physics, because this new piece of information about the nucleus will allow the most suitable nuclear models to be chosen from among the existing ones. The study of quasistationary nuclear states with excitation energy $\approx$550 MeV and their decays, like the study of hypernuclei, opens up the possibility of successfully constructing a theory of finite Fermi systems, while, on the other hand, it solves the problem of the low-energy ηN interaction, which has been intensively studied by theoreticians but not definitively solved, owing to the lack of experimental data.

The experiment, performed more than ten years ago at Brookhaven, to look for η nuclei in the reaction

$$\pi+A\to p+{}_{\eta}A' \tag{3}$$

near threshold did not give any definite result.[5] The observed peak in the energy spectrum of protons from the reaction $^{16}O(\pi^+,p)$ turned out to be lower than the predicted peak from the reaction $^{16}O(\pi^+,p)^{15}_{\eta}O$ by a factor of three. Without going into the details of the experiment, we note that the η-nucleus widths calculated in Ref. 3, on which the calculated heights of these peaks depend directly, have been subject to a considerable amount of criticism.[6,7] Another experiment on pion double charge exchange in the reaction

$$\pi^+ + {}^{18}O\to\pi^- + {}^{18}Ne,$$

performed at Los Alamos, revealed a resonance structure of the cross section for this reaction at an energy close to the η-meson production threshold,[8] but the small statistics did not permit the authors of that study to claim the discovery of η nuclei. Mention should also be made of the measurement of the cross section for the reaction $d+d\to\eta+{}^4He$ near threshold. At first no special features were found in the energy dependence of this cross section,[9] but later (apparently, under the influence of the results of experiments on the reactions $p+d\to\eta+{}^3He$ and $\pi^-+{}^3He\to\eta+T$; Refs. 10 and 11) the cross section was remeasured and an anomaly at threshold was found in it, which was taken as indirect evidence of the formation of a quasibound $\eta-{}^4He$ state.[12]

In the present study we discuss the problems associated with the existence of η nuclei and their production initiated by photons in the reaction

$$\gamma+A\to N+{}_{\eta}A' \tag{4}$$

as one of the most promising reactions for discovering η nuclei. It may be advantageous to search for η nuclei in the reaction (4) instead of (3), owing to the better background conditions in working with photon beams as compared with π-meson ones. Another advantage is the high predictability of the yield of the reaction (4) compared with that of (3), owing to the high uncertainty of the mechanism for the pion interaction with nuclei at the energies in question.

In this review we first analyze the available experimental and theoretical data on the interaction and production of η mesons, in order to confirm indirectly the possibility that superlight η nuclei exist. The main properties of η nuclei, such as their binding energy and lifetime, are studied as functions of the nuclear density, the number of nucleons in the nucleus, and the ηN scattering length. In Sec. 2 we study η-meson photoproduction on nucleons and nuclei at near-threshold energies of the incident photons. We construct a model for η photoproduction on protons and neutrons which reproduces the recent experimental data.[13,14] The amplitudes of the elementary processes obtained in this model are used for the theoretical study of meson photoproduction on p-shell nuclei with nucleon emission. The calculated cross sections for η-meson photoproduction on nuclei are compared with the results of calculations by other authors and also with the available experimental data. In the last section we give the theoretical justification for the model of η-nucleus photoproduction with nucleon emission and calculate the cross sections for producing η nuclei. The dependence of the cross sections on the main properties and states of the produced η nuclei and on the final-state interaction of the emitted nucleons is studied.

1. η NUCLEI AND THEIR PROPERTIES

1.1. The optical model for the interaction of η mesons with nuclei

At the present time there are two basic approaches to describing η nuclei. In one of them it is assumed that a slow η meson interacts with the nucleons of the nucleus exclusively via the production and decay of the $S_{11}(1535)$ isobar. As a result of this interaction, an excited nuclear state of the particle–hole type is formed, with the $S_{11}(1535)$ isobar playing the role of the particle. The properties of this excited state (its binding energy and lifetime) depend not only on the properties of the $S_{11}(1535)$ resonance, but also on its interaction with the nucleus.[7] In the other approach the interaction of a slow meson with the nucleons of the nucleus is assumed to be coherent and is described by an optical potential, as was done long ago in describing the pion–nucleus interaction. An important component of this approach is the amplitude of the low-energy ηN interaction, in particular, its critical characteristic such as the ηN scattering length a_0.

We shall use the concept of an optical potential to describe the meson–nucleus interaction. Neglecting two-nucleon absorption of the η meson in the nucleus, the optical potential at threshold ($\bar{q}_\eta \to 0$) can be written as[15]

$$2\mu U(r) = -4\pi\rho(r)(1+m_\eta/m_N)\cdot f(\eta N \to \eta N), \qquad (5)$$

with $\mu = m_\eta M/(m_\eta + M)$. Here M is the mass of the nuclear core, $\rho(r)$ is the spherically symmetric potential density, and $f(\eta N \to \eta N)$ is the amplitude of the elementary process, with

$$f(\eta p \to \eta p) = f(\eta n \to \eta n) \qquad (6)$$

according to the isotopic invariance of the strong interactions.

In contrast to πN scattering, at very low meson energies ηN scattering can be treated as pure S-wave scattering, owing to the dominance in its cross section, beginning at threshold, of the nucleon resonance $S_{11}(1535)$, and therefore

$$\lim_{q_\eta \to 0} f(\eta N \to \eta N) = a_0. \qquad (7)$$

To determine the complex η-nuclear interaction potential we use the free ηN scattering length (the formalism of the effective scattering length developed in Ref. 15 for π mesons cannot be applied directly here).

The next approximation will be that of uniform density. In (5), $\rho(r)$ is taken in the form

$$\rho(r) = \begin{cases} \dfrac{3}{4\pi r_0^3}, & r \leqslant R \\ 0, & r > R \end{cases} \qquad (8)$$

where

$$R = r_0 A^{1/3} \qquad (9)$$

is the radius of a nucleus containing A nucleons. This approximation is justified because we shall study only light nuclei, and the potential in (5) does not contain any terms depending on the gradient of the nuclear density.

Neglecting spin effects, the Schrödinger equation for the η nucleus will have the form

$$\left[-\frac{\nabla^2}{2\mu} + U(r)\right]\varphi_{n\ell}(\mathbf{r}) = E_{n\ell}\varphi_{n\ell}(\mathbf{r}) \qquad (10)$$

with complex energy eigenvalue

$$E_{n\ell} = \left(-\varepsilon - \frac{1}{2}i\Gamma\right)_{n\ell}, \qquad (11)$$

where ε and Γ are the binding energy and width of the level with quantum numbers n and ℓ. Using the expansion in Legendre polynomials $P_\ell(\cos\theta)$ to separate the wave function $\varphi_{n\ell}(\mathbf{r})$ into radial and angular parts,

$$\varphi_{n\ell}(\mathbf{r}) = \sum_{\ell=0}^{\infty} \frac{u_{n\ell}(r)}{r}\cdot P_\ell(\cos\theta).$$

we obtain the usual differential equation for $u_{n\ell}(r)$,

$$r^2 \ddot{u}_{n\ell}(r) + [2\mu r^2(E_{nl} + U(r)) - \ell(\ell+1)]u_{n\ell}(r) = 0, \qquad (12)$$

which for $\ell = 0$ has an elementary solution, and for $\ell > 0$ has analytic solutions in the form of Riccati functions. As usual, we obtain the energy-quantization condition by matching the logarithmic derivatives of the wave functions $\varphi_{n\ell}(\mathbf{r})$ at the boundary where the potential acts.

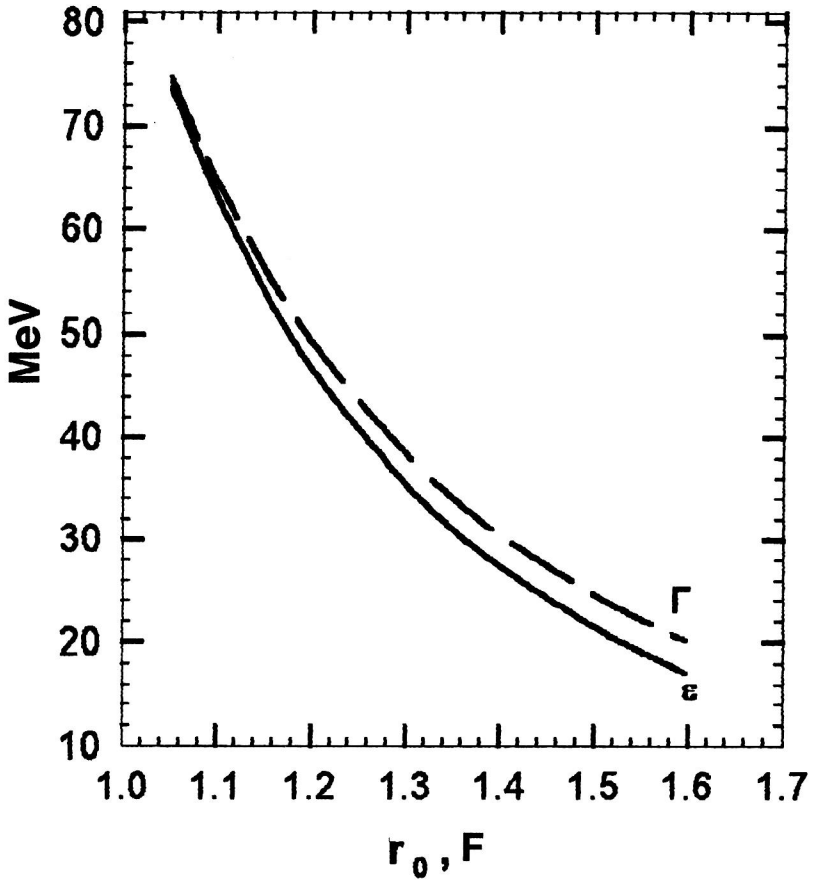

FIG. 1. Dependence of the binding energy ε and the level width Γ of the $1s$ state of the $^{16}_{\eta}$O nucleus on the radial parameter r_0 of the optical potential, calculated with the ηN scattering length $a_0=(0.717+i0.263)$ F.

1.2. The properties of η nuclei

In our model the properties of η nuclei will be determined by two basic parameters: the ηN scattering length a_0 and the radius R (9) of the potential. The strongest dependence will be that on the radial parameter r_0 [see Eqs. (5) and (8)]. The dependence of the binding energy and the width of the $1s$ level of the η nucleus $^{16}_{\eta}$O on the radial parameter for fixed a_0 is shown in Fig. 1. On the basis of general considerations about the strong-interaction range, it can be assumed that

$$1.3\,\text{F}<r_0<1.4\,\text{F}.$$

The resulting uncertainty in ε and Γ can be estimated from Fig. 1. For R (9) we take the equivalent nuclear radii R_{eq}, which are related to the corresponding rms radii as

$$R_{\text{eq}}^2=\frac{5}{3}\langle r^2\rangle. \tag{13}$$

For the nuclei that we shall consider here, the R_{eq} were taken without change from the table of Ref. 16, except for the ^{11}B nucleus, for which we took $r_0=1.35$ F (bearing in mind the remark of that author about the probable error in that quantity). Another important component of the potential U (5) will be the ηN scattering length. As already mentioned, the situation here is contradictory, and at present it is impossible to give preference to any particular result. In Fig. 2 we show the values of a_0 from most of the studies known to us[17–23] (see Ref. 22 for a more detailed review of these studies).

A quasibound state is possible in a complex potential only for particular relations between its real and imaginary parts. The calculated boundaries for the production of some η nuclei in the complex a_0 plane are shown in Fig. 2. To the right of these curves we have the values of a_0 which lead to the bound, lowest-lying states of the corresponding η–A systems. We see that the hypothetical existence of η nuclei heavier than $^{16}_{\eta}$O does not come into conflict with any of the values of a_0 obtained in the cited studies.

In discussing the possibility of η-nucleus production, the authors of Ref. 4 put a lower limit on the number of nucleons, $A\geq 12$, on the basis of the values of a_0 that they obtained. The corresponding curve in Fig. 2 gives a good illustration of this. In addition, there are quite a few studies whose results satisfy the conditions

$$|\text{Re}\,a_0|>0.55\,\text{F}, \quad |\text{Im}\,a_0|<0.4\,\text{F}$$

(Refs. 18–23), which allows η nuclei with fewer than 12 nucleons to exist (see Fig. 2). In extending the concept of an optical potential to nuclei with $A=3$, we calculated the boundary for producing $^{3}_{\eta}$He, taking into account the friability of its nucleon core ($R_{\text{eq}}=2.45$ F; Ref. 16). As can be seen from Fig. 2, some of the predicted values of a_0 remain to the right of this curve, thereby leaving open the possibility that superlight η nuclei exist up to $_{\eta}$D. This version is supported by the results of studies of near-threshold η-meson production reactions: $\gamma+\text{D}\to\eta+\text{D}$ (Ref. 24), $p+\text{D}\to\eta+^3\text{He}$ (Ref. 10), $\pi^-+^3\text{He}\to\eta+\text{T}$ (Ref. 11), $\text{D}+\text{D}\to\eta+^4\text{He}$ (Ref. 12),

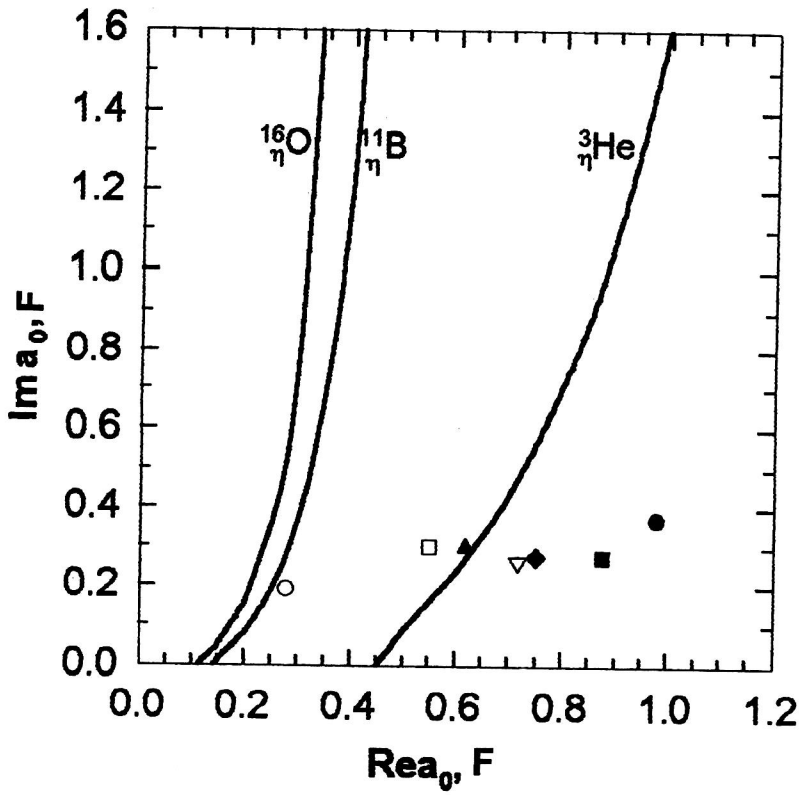

FIG. 2. Boundaries of the production of quasibound states for several η nuclei in the complex plane of the ηN scattering length. The figure shows the ηN scattering lengths obtained in the following studies: Ref. 17 (○), Ref. 18 (●), Ref. 19 (□), Ref. 20 (▲), Ref. 21 (■), Ref. 22 (▽), Ref. 23 (◆).

and $p+n\to\eta+\mathrm{D}$ (Ref. 25). As mentioned above, the measured cross sections of these reactions turned out to be anomalously large at the threshold or in its immediate vicinity. Among the explanations of this fact there are some[19,26] in which it is assumed that the reaction $p+\mathrm{D}\to\eta+{}^3\mathrm{He}$ occurs via an S-wave resonance with mass

$$M_R=M_{^3\mathrm{He}}+m_\eta-7\ \mathrm{MeV}/c^2$$

($7\ \mathrm{MeV}/c^2$ below the threshold for η-meson production in this reaction) and less certain width

$$\Gamma=5-25\ \mathrm{MeV}.$$

It is natural to interpret this resonance as the η nucleus ${}^3_\eta\mathrm{He}$ with binding energy and width

$$\varepsilon\approx 7\ \mathrm{MeV},\quad \Gamma\approx 15\ \mathrm{MeV}. \tag{14}$$

If the η-nuclear potential is constructed on the basis of the ηN scattering length from Ref. 21,

$$a_0=(0.880+i0.274)\ \mathrm{F}, \tag{15}$$

then from our model we find

$$\varepsilon=6.2\ \mathrm{MeV},\quad \Gamma=14.0\ \mathrm{MeV}. \tag{16}$$

We note that the value (15) for a_0 is not extreme compared with the others (see Fig. 2) and agrees, within the cited errors, with the results of other authors. Assuming that the characteristics[26] of the S-wave resonance via which the process $p+\mathrm{D}\to\eta+{}^3\mathrm{He}$ occurs and the properties (16) calculated for ${}^3_\eta\mathrm{He}$ do not coincide accidentally, of all the predicted scattering lengths preference can be given to the result (15) of Ref. 21. The properties of some η nuclei obtained on the basis of this value are given in Table I. The binding energy and widths are larger than those predicted in the earliest studies[3,4] for similar nuclei, but they are consistent with the results of Ref. 7 obtained in an alternative model of η nuclei with nonuniform density. In the same table we give the properties of η nuclei with $A<40$ calculated with the ηN scattering length

$$a_0=(0.717+0.263i)\ \mathrm{F} \tag{17}$$

from Ref. 22. The binding energies of the corresponding η nuclei differ considerably in the variants given, but (and this is particularly important) the widths of the studied quasibound η-meson–nucleus states, independently of the values of a_0 used in the calculations and the number of nucleons in the η nuclei, are all larger by about the same amount (see Table I), and significantly larger than the widths predicted in

TABLE I. Complex energy eigenvalues $E=(\varepsilon+i\Gamma/2)$ MeV in the model with a square-well potential.

Nucleus		$a_0=(0.880+0.274i)$ F	$a_0=(0.717+0.263i)$ F
${}^3_\eta\mathrm{He}$	1S	$6.2+7.00i$	$2.30+5.50i$
${}^4_\eta\mathrm{He}$	1S	$28.3+18.8i$	$17.5+16.85i$
${}^{11}_\eta\mathrm{B}$	1S	$38.1+18.0i$	$27.5+16.75i$
	1P	$17.4+12.4i$	$10.3+7.88i$
${}^{12}_\eta\mathrm{C}$	1S	$38.2+17.7i$	$28.0+16.65i$
	1P	$18.4+13.0i$	$10.6+9.13i$
${}^{15}_\eta\mathrm{N}$	1S	$40.7+17.9i$	$30.2+16.85i$
	1P	$21.9+14.6i$	$13.1+11.86i$
${}^{16}_\eta\mathrm{O}$	1S	$41.2+17.9i$	$30.6+16.82i$
	1P	$22.8+14.9i$	$13.9+12.36i$
${}^{40}_\eta\mathrm{Ca}$	1S	$51.4+19.4i$	$39.9+18.45i$
	1P	$38.8+18.5i$	$27.9+17.20i$
	2s	$15.2+16.6i$	$5.3+14.65i$

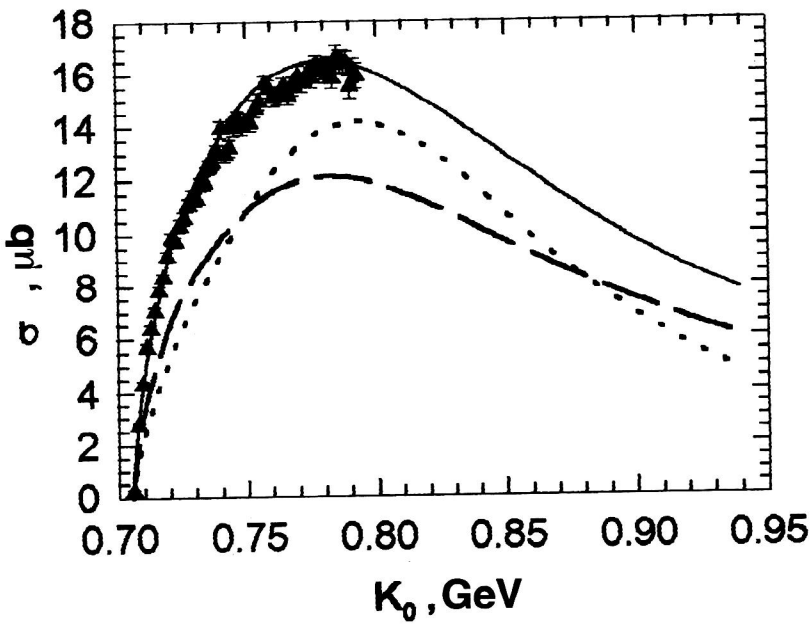

FIG. 3. Total cross sections for the processes $\gamma p \to \eta p$ (solid line) and $\gamma n \to \eta n$ (dashed line), calculated in the proposed model as a function of the photon energy. The dotted line is the result of the fit to the cross section for the process $\gamma p \to \eta p$ from Ref. 36 (solution A2). The experimental data on the cross section for the process $\gamma p \to \eta p$ are taken from Ref. 13.

Refs. 3 and 4. Consequently, the levels in multilevel η nuclei can overlap strongly, leading ultimately to a decrease of the lifetime of these nuclei.

Thus, on the one hand, the recent theoretical studies performed by the coupled-channel method to determine the ηN scattering lengths[20–23] give values at which η-meson–nucleus bound systems with $A<3$ can exist up to ${}_{\eta}$D (see Fig. 2). On the other hand, there have long been difficult-to-explain data on the threshold production of η mesons on few-nucleon systems independently of the type of incident particle. If we assume that all these reactions proceed through the formation and decay of the corresponding η nuclei (subthreshold resonances), then the behavior of their cross sections at threshold can, in principle, be explained. As yet there is no alternative to the existence of η nuclei with the number of nucleons $A>16$ (see Fig. 2).

The existence of superlight η nuclei has been suggested earlier,[18,19,27,28] but these suggestions turned out to be almost fantastic. More recently, the existence of superlight η nuclei has been justified in theoretical studies performed by the Green-function technique.[29–31] This approach eliminates the problem of non-Hermiticity of the Hamiltonian with a complex potential, existing in our treatment. It follows from the present study and from the cited literature that the lifetimes of light and intermediate η nuclei are several times smaller than the values predicted in the pioneering studies of Refs. 3 and 4, and are sufficient only for them to be manifested as a special type of nuclear threshold resonance, which makes them rather difficult to detect.

To study the photoproduction of η nuclei it is necessary to have information about η-meson photoproduction on nucleons and nuclei. This is the subject of the following section.

2. PHOTOPRODUCTION OF η MESONS ON NUCLEONS AND NUCLEI

2.1. Photoproduction of η mesons on nucleons

The photoproduction of η mesons on hydrogen nuclei,

$$\gamma + p \to \eta + p, \tag{18}$$

has now been studied for three decades.[33,34] Recent experiments[13,35] have qualitatively confirmed the results of the earlier measurements. The total cross section for the reaction (18) grows rapidly beginning at threshold, reaching the maximum value 15–17 μb at $K_0 = 800$ MeV, and then falls, as after a resonance. No other pronounced resonances are seen in the cross section for this process up to a photon energy of 2200 MeV (see Ref. 36). The nearly isotropic meson angular distribution[13] in the process (18) and the closeness of the mass of the $S_{11}(1535)$-resonance mass to its invariant threshold energy indicate that this resonance plays a leading role also in η-meson photoproduction on nucleons. The multiparameter analysis of (18) in a wide range of energies using a large number of resonances which was performed more than 20 years ago[36] poorly reproduces the results of new precision measurements of the cross section for this process near threshold[13] (see Fig. 3) and cannot be used directly. A more detailed analysis of this reaction near threshold[37,38] showed that it is sufficient to include only the three resonance nucleon states

$$S_{11}(1535), \quad P_{11}(1440), \quad D_{13}(1520) \tag{19}$$

and the small contribution to the cross section from the Born terms and graphs with vector-meson exchange.[39,40] Without going into the details of the threshold photoproduction of η mesons on nucleons, in that study the amplitude for the process (18) was described by a purely isobaric model including the three resonances (19), with the resonance multipole amplitudes parametrized as in Ref. 36 but with different param-

TABLE II. Parameters for resonance multipoles in the amplitude of the process $\gamma p \to \eta p$. The quantities γ^E and γ^M are expressed in terms of the product of partial widths of the corresponding resonances as in Ref. 36.

Resonance	M_R, MeV	Γ, MeV	γ^E, MeV	γ^M, MeV	Γ_η/Γ	Γ_π/Γ
S_{11}	1537	160	2.05	-	0.5	0.4
P_{11}	1440	350	-	0.25	-	-
D_{13}	1518	100	0.04	0.35	-	-

eters. The parameter values giving a good description of the Mainz cross-section measurements (see Fig. 3) are given in Table II.

To describe η-meson photoproduction on neutrons,

$$\gamma + n \to \eta + n, \tag{20}$$

the resonance multipole amplitudes were expressed in terms of the corresponding multipole amplitudes of the process (18) as follows:

$$S_{11}: \quad E_{0^+}^{(n)} = -0.848 E_{0^+}^{(p)},$$

$$P_{11}: \quad M_{1^-}^{(n)} = -0.722 M_{1^-}^{(p)},$$

$$D_{13}: \quad E_{2^-}^{(n)} = -0.538 E_{2^-}^{(p)}, \quad M_{2^-}^{(n)} = -2.2 M_{2^-}^{(p)}, \tag{21}$$

following the recommendations of Ref. 1. In Figs. 3 and 4 we show the cross sections for the process (20). They are significantly smaller than those for (18) and agree with the result

$$\sigma(\gamma n \to \eta n) \approx 0.70 \sigma(\gamma p \to \eta p), \tag{22}$$

obtained in Refs. 14 and 40 by a combined analysis of the experimental cross sections for the processes $\gamma p \to \eta p$ and $\gamma + D \to \eta + X$ at photon energies near threshold. We note that the predicted differential cross sections for the process $\gamma n \to \eta n$ are more anisotropic than those for $\gamma p \to \eta p$ (Fig. 4).

The model of η-nucleus photoproduction is based on knowledge about meson photoproduction on nuclei with the knockout of a single nucleon. These reactions have not yet been sufficiently studied either experimentally or theoretically, and therefore such reactions on p-shell nuclei must be studied in detail.

2.2. The amplitude of the reaction $A(\gamma, \eta N)A'$ on p-shell nuclei

The study of exclusive $(\gamma, \eta N)$ reactions is important, both for explaining the mechanisms of meson photoproduction on nuclei and for studying the properties of the nuclei themselves. The reaction of η-meson photoproduction on a nucleus A with emission of a nucleon N can be written as

$$\gamma(k, \varepsilon_\lambda) + A_i(Q_i) \to \eta(q) + N(p) + A_f(Q_f), \tag{23}$$

where we use $k = \{k_0, \mathbf{k}\}$, $q = \{q_0, \mathbf{q}\}$, $p = \{p_0, \mathbf{p}\}$, $Q_i = \{Q_{0i}, \mathbf{Q}_i\}$, and $Q_f = \{Q_{0f}, \mathbf{Q}_f\}$ to denote the four-momenta of the corresponding particles, and λ is the photon polarization index. Using the technique of second quantization and taking into account the antisymmetry of the wave functions of the initial (A_i) and final (A_f, N) systems of nucleons, the amplitude of the reaction (23) can be reduced to the form

$$\langle f | \hat{T}_{\gamma\eta} | i \rangle = \sqrt{A} \left\langle \psi_f \left| \sum_{n=1}^{A} \Phi_N^*(x_A) e^{i(\mathbf{k}-\mathbf{q})\mathbf{r}_n} \mathbf{t}_n \boldsymbol{\varepsilon}_\lambda \right| \psi_i \right\rangle. \tag{24}$$

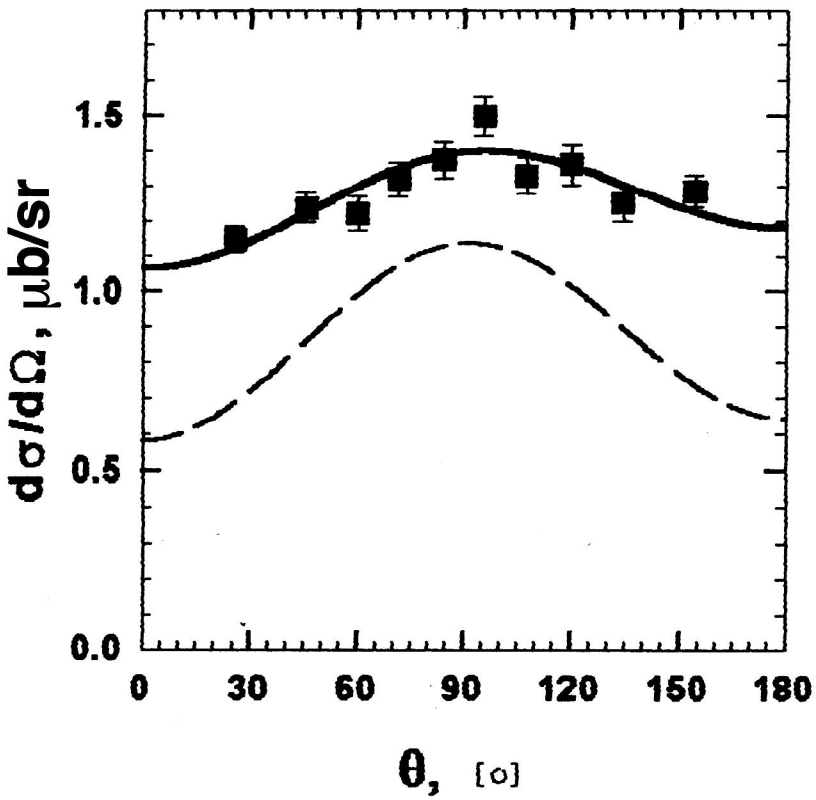

FIG. 4. Differential cross sections for the processes $\gamma p \to \eta p$ (solid line) and $\gamma n \to \eta n$ (dashed line) at $K_0 = 789.9$ MeV. The notation is the same as in Fig. 3. The experimental data on the differential cross section for the process $\gamma p \to \eta p$ are taken from Ref. 13.

Here $|\Psi_i\rangle$ and $|\Psi_f\rangle$ are the wave functions of the nucleus A_i consisting of A nucleons and the nucleus A_f consisting of $(A-1)$ nucleons. The operator $\hat{t}_n^{\lambda}=\hat{t}_n\cdot\bar{\varepsilon}_{\lambda}$ is the operator for η-meson photoproduction on a nucleon of the nucleus, which in the impulse approximation is equal to the operator for photoproduction on a free nucleon and has the form

$$t_n^{\lambda}=[K^S+K^V\tau_3+\mathbf{L}^S\boldsymbol{\sigma}+\mathbf{L}^V\boldsymbol{\sigma}\tau_3]_n^{\lambda},$$

where $\boldsymbol{\sigma}$ and $\tau=\{\tau_1,\tau_2,\tau_3\}$ are respectively the spin and isospin operators of the nucleon, and s and v indicate the isoscalar and isovector parts of the amplitude. $\Phi_N(x_A)=\Phi_p^{(-)}(\mathbf{r}_A)\chi_{\alpha}(s_A)\chi_{\beta}(t_A)$ is the wave function of the emitted nucleon, where x_A is the set of variables $\{r_A,s_A,t_A\}$. Isolating the last term in the amplitude from the sum over n, we find

$$\langle f|\hat{T}_{\gamma\eta}|i\rangle=\sqrt{A}\langle\psi_f|\Phi_N^*(x_A)e^{i(\mathbf{k}-\mathbf{q})\mathbf{r}_A}\mathbf{t}_A\boldsymbol{\varepsilon}_{\lambda}|\psi_i\rangle+\Delta, \quad (25)$$

$$\Delta=\sqrt{A}\left\langle\psi_f\left|\sum_{m=1}^{A-1}\Phi_N^*(x_A)e^{i(\mathbf{k}-\mathbf{q})\mathbf{r}_m}\mathbf{t}_m\boldsymbol{\varepsilon}_{\lambda}\right|\psi_i\right\rangle. \quad (26)$$

The first term in the amplitude (25) describes quasifree meson photoproduction on nuclei, when the nucleon emitted from the nucleus carries off all the momentum transferred in the meson photoproduction. The residual nucleus A_f remains a spectator,[41] moving before and after the reaction with unchanged momentum

$$\mathbf{Q}_f=-\mathbf{p}_i, \quad (27)$$

and $\mathbf{p}_i$ is the momentum of the nucleon in the nucleus before the meson is produced on it. As long as $|\mathbf{Q}_f|<250\,\text{MeV}/c$, this part of the amplitude is much larger in magnitude than $|\Delta|$ in (26). As $|\mathbf{Q}_f|$ increases, the part of the amplitude responsible for quasifree photoproduction decreases sharply, and so the contribution to the cross section from the rest of the amplitude Δ becomes important. Equation (26) can be interpreted as the amplitude for coherent η photoproduction on $(A-1)$ nucleons of the nucleus, including the emitted nucleon. This part of the amplitude has not yet been well studied, but it is known that if $|\mathbf{Q}_f|$ falls in the range of the most probable nucleon momentum distribution in the nucleus [this relation is evident from (27)], then the quantity Δ in the amplitude (25) can be neglected in calculating the cross sections.[41–43] Below, for the reactions (23) we shall study the kinematical region in which $50\,\text{MeV}/c<|\mathbf{Q}_f|<250\,\text{MeV}/c$, taking $\Delta=0$ in the amplitude (25).

If η mesons are produced on s-shell nucleons, then the nucleus A_f in the reaction (23) remains in an excited state with configuration

$$|(1s)^3;\quad (1p)^{A-4}\rangle,$$

corresponding to a "hole" in the s shell. Such states are treated in the nuclear shell model as having an excitation quantum of at least $1\hbar\omega$ in the fermionic system, which is unnecessarily complicated in the realization of the calculations of our amplitude (25). Using the shell model with intermediate coupling,[44,45] which gives a good description of the ground and low-lying excited states of p-shell nuclei in terms of only the state of the nucleons in the outer shell, we will thereby be neglecting meson photoproduction on the nucleons of s-shell nuclei in reactions of the form (23).

Let us now consider the $(\gamma,\eta p)$ reaction on the ^{12}C nucleus:

$$\gamma(k,\lambda)+{}^{12}\text{C}(Q_i)\to\eta(q)+p(p_f)+{}^{11}\text{B}^*(Q_f). \quad (28)$$

In the nuclear model under discussion, it is sufficient to take the ^{12}C wave function in the approximation where its spatial part is most symmetric:

$$\psi_i(J_i,M_i)=|(1s)^4;(1p)^8[44]L_i=0,S_i=0,T_i=0\rangle, \quad (29)$$

where J_i is the nuclear spin with projection M_i; L_i, S_i, and T_i are the total orbital, spin, and isospin momenta of the nucleons in the p shell, and $[44]=[f_i]$ is the Young scheme[46] for the same nucleons. The amplitude of the reaction (28) in the impulse approximation can now be written as (the LS representation)

$$\begin{aligned}\langle f|\hat{T}_{\gamma\eta}|i\rangle=\sqrt{8}\sum_{\substack{L,S,T,[f],L_f,S_f,T_f\\ L^z,S^z,T^z,L_f^z,S_f^z,m,\tau}} a_{LST}^{[f]}\cdot\delta_{S_f,S}\cdot\delta_{L_f,L}\cdot\delta_{T_f,T}\\ \cdot\delta_{[f_f],[f]}\cdot\langle L_fL_f^z,1m|00\rangle\left\langle S_fS_f^z,\frac{1}{2}\xi\right|00\right\rangle\\ \times\left\langle T_fT_f^z,\frac{1}{2}\tau\right|00\right\rangle\\ \times\langle L_fL_f^z,S_fS_f^z|J_fM_f\rangle H_{\xi\tau}^{\alpha\beta}(\lambda)\cdot\tilde{D}_{1m}(\mathbf{Q}_f), \quad (30)\end{aligned}$$

where $\langle\ldots,\ldots|\ldots\rangle$ are the usual Clebsch–Gordan coefficients,

$$H_{\xi\tau}^{\alpha\beta}(\lambda)=\sum_{s,t}\chi_{\beta}^+(t)\chi_{\alpha}^+(s)t_A^{\lambda}(s,t)\chi_{\xi}(s)\chi_{\tau}(t), \quad (31)$$

and $a_{LST}^{[f]}$ are the one-particle fractional-parentage coefficients of the p-shell nucleus. For a selected configuration of the form (29), the only nonzero fractional-parentage coefficient is

$$a_{1\,1/2\,1/2}^{[43]}=1,$$

and $\tilde{D}_{1m}(\mathbf{Q}_f)$ is the overlap integral. In the plane-wave approximation for the wave function of the outgoing meson it has the form

$$\tilde{D}_{1m}(\mathbf{Q}_f)=\int d^3r\Phi_p^{(-)*}(\mathbf{r})e^{i(\mathbf{k}-\mathbf{q})\mathbf{r}}\varphi_{1m}(\mathbf{r}), \quad (32)$$

where $\varphi_{1m}(\mathbf{r})$ is the spatial part of the nucleon wave function in the p shell of the ^{12}C nucleus, and $\Phi_p^{(-)}(\mathbf{r})$ is the wave function of the emitted nucleon interacting with the nucleus. For proton kinetic energy $T_p>60\,\text{MeV}$ the interaction with the nucleus can be estimated fairly accurately by means of simple models, in particular, by taking the wave function $\Phi^{(-)}$ of an intranuclear nucleon in the form

$$\Phi_{p_f}^{(-)}(\mathbf{r})=\exp\left[\frac{1}{\beta}(-iV_R+V_I)d(\mathbf{r})\right]\exp(i\mathbf{p}_f\mathbf{r}), \quad (33)$$

which is the solution of the Schrödinger equation with homogeneous optical potential $V(\mathbf{r})=V_R+iV_I$. Here β is the

velocity and $d(\mathbf{r})$ is the length of the proton trajectory in the nucleus. Following Ref. 47, we have assumed that it is classical, i.e., parallel to the momentum $\mathbf{P}_f$. To the extent that the wave function (33) is suitable only for calculations with uniform nuclear density, we have factorized the quantity $\tilde{D}_{1m}$ given by (32), using the mean-value theorem, as

$$\tilde{D}_{1m}=fD_{1m},$$

$$f(V_R,V_I)=\int d^3x\frac{3}{4\pi R^3}\exp\left[\frac{1}{\beta}(-iV_R+V_I)d(\mathbf{x})\right]$$
$$=(2z^3)^{-1}[6(1+z)e^{-z}+(3z^2-3y^2$$
$$-6y-6)e^{-y}+y(3z^2-y^2)],$$
$$z=2R\left[\frac{iV_R-V_I}{\beta}\right],\quad y=RA^{-1/3}\left[\frac{iV_R-V_I}{\beta}\right]. \tag{34}$$

In calculating this integral we have used the fact that a nucleon emitted from the outer layer of the nucleus of thickness $RA^{-1/3}$ facing the emission direction must not undergo any interaction. The remaining integral

$$D_{1m}(\mathbf{Q}_f)=\int e^{i(\mathbf{k}-\mathbf{q}-\mathbf{p})\mathbf{r}}\varphi_{1m}(\mathbf{r})d^3r$$

is the overlap integral in the plane-wave approximation for the emitted nucleon and meson. By using oscillator single-particle nuclear functions $\varphi_{1m}(\mathbf{r})$, as was done in the calculations, this integral can be expressed in terms of elementary functions. As a result, the effect of the interaction between the proton and the residual nucleus in our case for the reaction (23) will be expressed as a factor $|f|^2$ in front of the differential cross section calculated in the plane-wave approximation. The values of the real and imaginary parts of the nucleon–nucleus optical potential $V(x)$ were taken from Ref. 41 (set 3). It should be noted that the solution (33) adequately reflects the interaction of the nucleons with the nucleus only for nucleon energies above 60 MeV (Ref. 47). At energies below 40 MeV, the energy of the giant resonance, the effect of the nucleon–nucleus interaction becomes strongly dependent on the state of the residual nucleus and cannot be taken into account in simple models.

So far, nothing has been said about the states in which the nuclei can be found after nucleon emission from the p shell. In the nuclear model under consideration it is possible to take into account the ground and low-lying excited states of normal parity. For example, for the reaction (28) these may be the following three states:

(i) the ground state with excitation energy $\varepsilon=0$,

$$^{11}\mathrm{B}(J^P=(3/2)^-,\ T=1/2); \tag{35}$$

(ii) the first and second excited states

$$^{11}\mathrm{B}^*(J^P=(1/2)^-,\ T=1/2), \tag{35a}$$

$$^{11}\mathrm{B}^*(J=(3/2)^-,\ T=1/2), \tag{35b}$$

with excitation energies $\varepsilon=2.12$ MeV and $\varepsilon=5.02$ MeV, respectively. We shall now discuss the cross sections for meson photoproduction on nuclei with nucleon knockout.

2.3. The cross sections for $A(\gamma,\eta N)A$ reactions

Let us consider the reaction (28) with the residual nucleus in the ground state (35):

$$\gamma+{}^{12}\mathrm{C}\to\eta+p+{}^{11}\mathrm{B}_{\mathrm{g.s.}}. \tag{36}$$

The differential cross section for this reaction, averaged over the photon polarizations and summed over the polarizations of the final particles, will have the form

$$\frac{d^3\sigma}{d\Omega_\eta d\Omega_p dq_0}=\frac{64}{9}K_3\sum_\lambda(|K^p(\lambda)|^2+|\mathbf{L}^p(\lambda)|^2)F(\mathbf{Q}_f)|f|^2, \tag{36a}$$

where $K^p=K^s+K^v$ and $\mathbf{L}^p=\mathbf{L}^s+\mathbf{L}^v$; the quantity $F(\mathbf{Q}_f)$ is the response function, apart from a constant. In our case it is

$$F(\mathbf{Q}_f)=\pi^{3/2}r_0^3(\mathbf{Q}_f r_0)^2\exp(-\mathbf{Q}_f^2r_0^2), \tag{37}$$

where $\mathbf{Q}_f=k-q-p_f$, r_0 is the oscillator parameter, which for ^{12}C was taken to be 1.67 F,

$$K_3=(2\pi)^{-5}\frac{|\mathbf{q}|q_0\mathbf{p}_f^2p_{0f}Q_{0f}}{|\mathbf{p}_f|Q_{0f}-p_{0f}(|\mathbf{k}-\mathbf{q}|\cos\theta-|\mathbf{p}_f|)} \tag{38}$$

is the kinematical factor for the distribution $d^3\sigma/d\Omega_\eta d\Omega_p dq_0$, and θ is the angle between the momenta $\mathbf{k}-\mathbf{q}$ and $\mathbf{p}_f$. The calculated differential cross section (36a) is shown in Fig. 5 along with the results of the calculation of the same cross sections from Refs. 48 and 49. The shape and value of the calculated distribution are in good agreement with the results of Ref. 49. As in that study, our impulse approximation has also been "relativized," owing to the use of the one-nucleon photoproduction operator $\hat{t}^\lambda$ in a form allowing the full inclusion of the intranuclear motion of the nucleons while preserving the gauge invariance of the nuclear photoproduction amplitude as a whole.[50] The calculated effect of the interaction of the emitted proton with the residual nucleus is close to that which the authors of Ref. 49 obtain for the same reaction.

Substituting $J_f=1/2$ and $T_f=1/2$ into the amplitude (29), we obtain the differential cross section for the $(\gamma,\eta p)$ reaction on ^{12}C with excitation of the first level (35a) in the ^{11}B nucleus:

$$\frac{d^3\sigma}{d\Omega_\eta d\Omega_p dq_0}=\frac{32}{9}K_3\sum_\lambda(|K^p(\lambda)|^2+|\mathbf{L}^p(\lambda)|^2)F(\mathbf{Q}_f)|f|^2. \tag{39}$$

It is not always possible to isolate the residual nucleus of a reaction of the type (23) according to the excitation energies, because the measured particle distributions in $(\gamma,\eta N)$ reactions are sums from reactions with different states of the final nuclei. The differential cross section for the reaction (28) with the residual nucleus in all possible bound states can be written as

$$\frac{d^3\sigma}{d\Omega_\eta d\Omega_p dq_0}=K_3\sum_\lambda(|K^p(\lambda)|^2+|\mathbf{L}^p(\lambda)|^2)F(\mathbf{Q}_f)|f|^2$$
$$\cdot\left[\frac{64}{9}(1+\alpha)+\frac{32}{9}(1+\beta)\right], \tag{40}$$

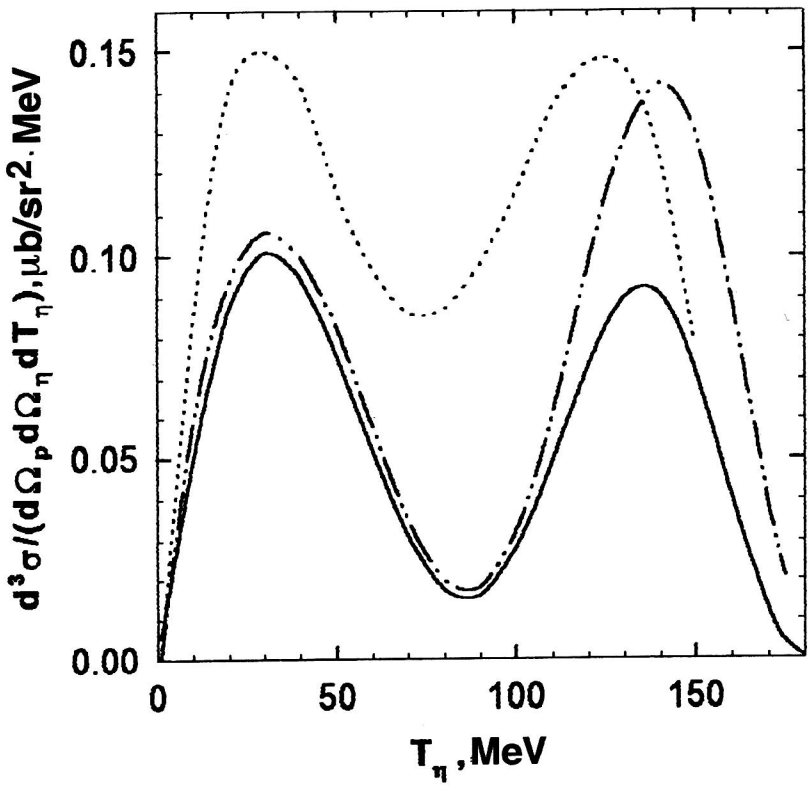

FIG. 5. Differential cross section for the reaction $^{12}C(\gamma,\eta p)^{11}B_{g.s.}$ for photon energy $K_0=750$ MeV and meson and proton emission angles $\theta_\eta=20°$ and $\theta_p=15°$ in a single plane as a function of the η-meson energy in the lab frame. The solid lines are the result obtained in the present study. The dot–dash and dotted lines are the results for the calculated cross section from Refs. 48 and 49, respectively.

$$\alpha=\frac{1}{S_\alpha(0)}\sum_\varepsilon S_\alpha(\varepsilon),\quad \beta=\frac{1}{S_\beta(2.13)}\sum_\varepsilon S_\beta(\varepsilon),$$

where $S_\alpha(0)$ and $S_\alpha(\varepsilon)$ are the spectroscopic factors of nucleons[45] of the ground and excited states of the ^{11}B nucleus with quantum numbers $J^pT=(3/2)^-1/2$, and $S_\beta(\varepsilon)$ is the same for states of ^{11}B with $J^pT=(1/2)^-1/2$. The values of α and β for the reaction (28) can be taken from Ref. 45:

$$\alpha=\frac{0.756}{2.5}\approx 0.3,\quad \beta=0.$$

Equation (40) can be used at photon energies somewhat above threshold, so that the mass (excitation energy) of the residual nucleus does not strongly affect the value of the cross section. Otherwise, the cross sections for reactions with different excitation levels of the final nucleus would have to be calculated separately with different kinematical factors K_3.

The nucleus with a filled $1p$ shell, ^{16}O, has a wave function similar to that in (29) for the ^{12}C nucleus with one-particle fractional-parentage coefficients equal to unity. Therefore, the differential cross section for the reaction

$$\gamma+{}^{16}O\rightarrow\eta+p+{}^{15}N_{g.s.} \tag{41}$$

is calculated by using the algorithm for calculating the cross sections for the reaction (28). As a result, we obtain

$$\frac{d^3\sigma}{d\Omega_\eta d\Omega_p dq_0}=\frac{16}{3}K_3\sum_\lambda\left(|K^p(\lambda)|^2+|\mathbf{L}^p(\lambda)|^2\right)F(\mathbf{Q}_f)\cdot|f|^2. \tag{41a}$$

The oscillator parameter r_0 for ^{16}O was taken to be 1.80 F. The result of the calculation is shown in Fig. 6 along with the calculated results for the same cross section from Ref. 49. It is interesting that the cross section for the reaction (41) turns out to be smaller than that for the reaction (36) and that for the $(\gamma,\eta p)$ reaction on ^{16}O:

$$\gamma+{}^{16}O\rightarrow\eta+p+{}^{15}N^*((3/2)^-,1/2), \tag{42}$$

with excitation of the level of energy $\varepsilon=6.3$ MeV in the residual nucleus ^{15}N. It can be written as

$$\frac{d^3\sigma}{d\Omega_\eta d\Omega_p dq_0}=\frac{32}{3}K_3\sum_\lambda\left(|K^p(\lambda)|^2+|\mathbf{L}^p(\lambda)|^2\right)F(\mathbf{Q}_f)\cdot|f|^2. \tag{42a}$$

There is no information available about other excited states of the ^{15}N nucleus with the quantum numbers of the ground state. As a result, the cross sections for the $(\gamma,\eta p)$ reaction on ^{12}C and ^{16}O will be roughly the same, despite the considerable difference in the numbers of nucleons in the $1p$ shells of these nuclei.

In its region of applicability ($T_p>60$ MeV), the simple model of the nucleon–nucleus interaction that we have used leads only to a decrease of the cross section for reactions like (23), both in the absence of a real part of the optical potential and when it is present (see Fig. 6). If as the criterion we take the effect of the interaction of the emitted proton with the ^{15}N nucleus obtained in Ref. 49, then it is preferable in our simple model to choose the nucleon–nucleus potential to be purely imaginary (see Fig. 6). Therefore, in what follows, if not stated otherwise, we shall take $V_R=0$ in Eq. (34) for f.

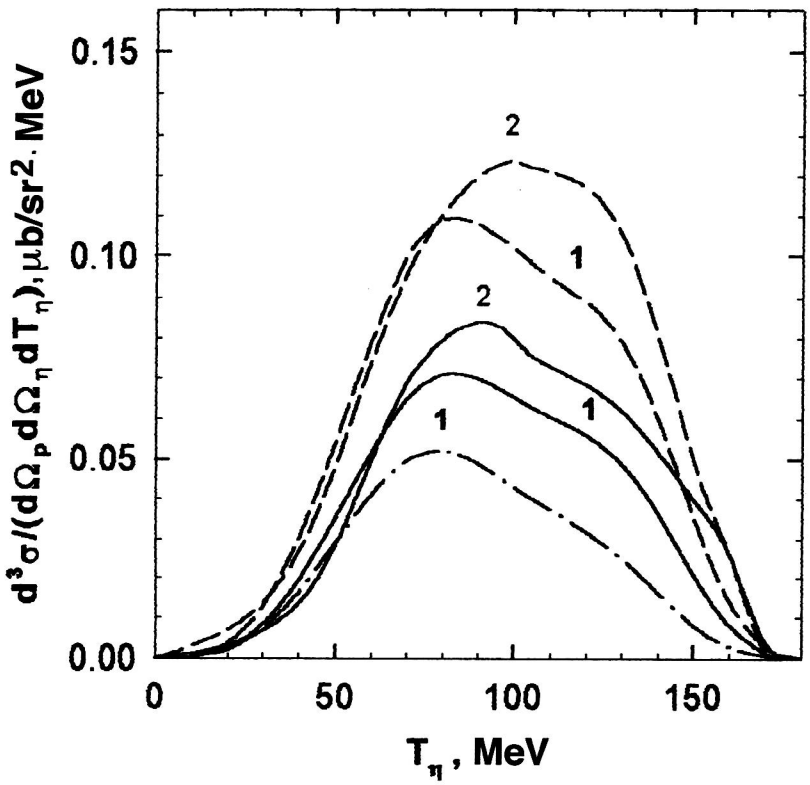

FIG. 6. Differential cross section for the reaction $^{16}O(\gamma,\eta p)^{15}N_{g.s.}$ for photon energy $K_0=750$ MeV and meson and proton emission angles $\theta_\eta=30°$ and $\theta_p=30°$ in a single plane as a function of the η-meson energy in the lab frame. Curves 1 were calculated in the present study, neglecting the final-state interaction (dashed line) and including the proton interaction in the final state, with (dot–dash line) and without (solid line) the real part of the optical potential. Curves 2 are the same cross section calculated in Ref. 49 with (solid line) and without (dashed line) the proton interaction in the final state.

If the simple shell model with a harmonic-oscillator potential is used to describe the nucleus ^{4}He with a closed $1s$ shell, for the cross section of the reaction

$$\gamma+{}^4\mathrm{He}\to\eta+p+T \tag{43}$$

we easily obtain an expression which in the notation of (37) and (38) can be written as

$$\frac{d^3\sigma}{d\Omega_\eta d\Omega_p dq_0}=8K_3\sum_\lambda(|K^p(\lambda)|^2+|L^p(\lambda)|^2)\frac{F(\mathbf{Q}_f)}{(\mathbf{Q}_f r_0)^2}|f|^2, \tag{43a}$$

with oscillator parameter $r_0=1.38$ F for ^{4}He. The translational noninvariance of the oscillator wave functions used for the nuclei was taken into account in these calculations by replacing the oscillator parameter r_0 by

$$\tilde{r}_0^2=r_0^2\frac{A}{A-1} \tag{44}$$

for each of the reactions discussed.

The expressions for the cross sections of $(\gamma,\eta n)$ reactions on the nuclei in question are the same as the expressions for the cross sections of $(\gamma,\eta p)$ reactions. Among the various distributions of products of the reactions (23) we shall use the distribution $d^3\sigma/d\Omega_\eta d\Omega_p dT_p$, for which we easily obtain the corresponding kinematical factor

$$\tilde{K}_3=(2\pi)^{-5}\frac{\mathbf{q}^2|\mathbf{p}_f|P_{0f}Q_{0f}q_0}{|\mathbf{q}|Q_{0f}-q_0(|\mathbf{k}-\mathbf{p}_f|\cos\tilde{\theta}-|\mathbf{q}|)},$$

where $\tilde{\theta}$ is the angle between the momenta $\mathbf{k}-\mathbf{p}_f$ and $\mathbf{q}$.

The prescription given in Ref. 48 was also used to estimate the cross sections for inclusive η-meson photoproduction on ^{12}C and ^{16}O nuclei. The total cross section for the reaction $^{12}C(\gamma,\eta)X$ calculated in the plane-wave approximation is compared with the experimental one[14] from threshold to $K_0=790$ MeV in Fig. 7. The insignificant excess of the calculated value over the experimental one at $K>700$ MeV leaves only 20–25% for the effect of the final-state interaction, which lowers the cross section. The twofold excess of the distribution $d^2\sigma/d\Omega_\eta dq_0$ that we have calculated at $K_0=720$ MeV and $\theta_\eta=10°$ over the result of the analogous calculation from Ref. 51 can be partially explained by the fact that these calculations include η-meson production via the $S_{11}(1535)$ isobar and its interaction with the nucleus. Finally, the result of our calculation of the cross section $d^2\sigma/d\Omega_\eta dq_0$ for the reaction $^{16}O(\gamma,\eta)X$ at $K_0=800$ MeV and $\theta_\eta=25°$ is almost 3 times higher than the corresponding result of Ref. 52. This discrepancy cannot be eliminated even by choosing a more suitable cross section for η-meson photoproduction on the neutron than the one used in Ref. 52.

3. PHOTOPRODUCTION OF LIGHT η NUCLEI

3.1. The model of photoproduction of η nuclei

It is possible for η nuclei to appear in various nuclear reactions occurring with η-meson production, when the latter is "attached" to the nuclear reaction products as a result of the attractive interaction. That is, the photoproduction of η nuclei can occur according to the scheme

$$\gamma+A\to\eta+A'+\ldots\to{}_\eta A'+\ldots,$$

where A' is a nuclear fragment having small velocity relative to the η meson. The simplest reaction to study theoretically is that of η photoproduction on a nucleus with the production of only two nuclear fragments, in particular, when one of them is simply a nucleon:

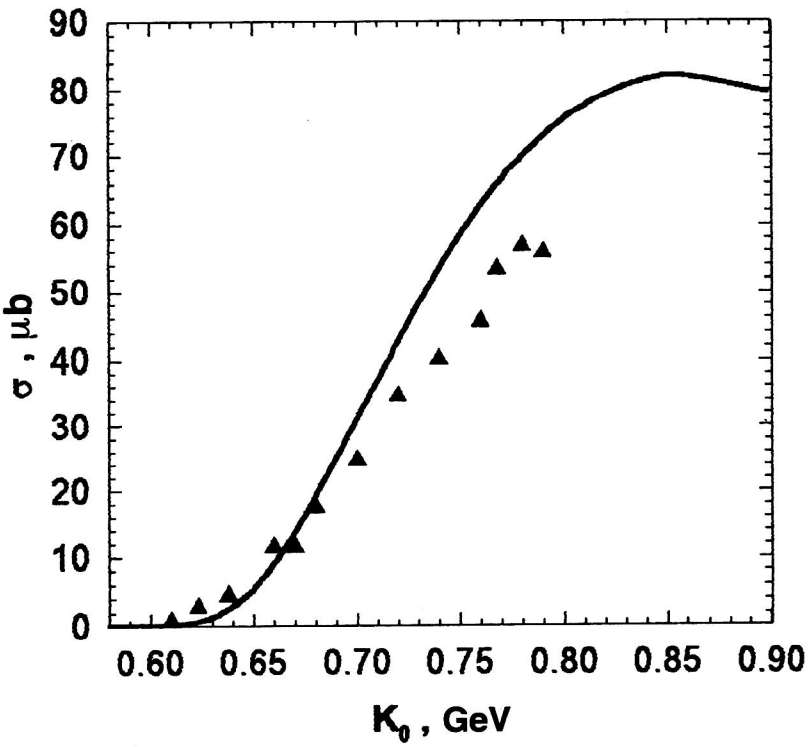

FIG. 7. Dependence of the total cross section for the reaction $^{12}C(\gamma,\eta)X$ on the incident γ energy. The experimental data are taken from Ref. 14.

$\gamma+A\rightarrow N+{}_{\eta}A'$.

The first studies to estimate the probability of η-nucleus production in the reaction (4) (Refs. 53 and 54) raised a number of questions related to the inadequate justification of the results of the calculation. At the present time, when η nuclei are becoming more real than hypothetical, it has become necessary to justify the models for their photoproduction in the reaction (4) in more detail. The η-nucleus production mechanism is shown by the graph in Fig. 8. According to the theory of scattering on two potentials,[55] the amplitude for the reaction (4) can be written as the sum of two amplitudes, one with the photoproduction potential and the other with the potential for meson–nucleus scattering. Since in photoproduction the "species" of particle changes, of the two amplitudes describing the scattering on two potentials, only one remains in photoproduction: that for meson photoproduction on the nucleus, in which the wave function of the emitted meson is replaced by that of the η meson interacting with the nucleus A_f (Ref. 55). Furthermore, the formation of the η-meson–nucleus quasiequilibrium state occurs over a finite time, the knocked-out nucleons are fast [eliminating the threshold for the reaction (4)], and the nucleon final-state interaction can be treated as for ordinary nuclei.

Thus, the mechanism for η-nucleus photoproduction in reactions like (4) is taken to be quasifree photoproduction of η mesons on the corresponding nuclei. The approximations associated with this mechanism will be discussed in the following section.

3.2. Photoproduction of superlight η nuclei

Following the above discussion, we assume that superlight η nuclei can exist and study ${}^3_{\eta}$He and ${}_{\eta}$T photoproduction in the reactions

$$\gamma+{}^4\text{He}\rightarrow p+\eta T, \tag{45}$$

$$\gamma+{}^4\text{He}\rightarrow n+{}^3_{\eta}\text{He}. \tag{46}$$

According to the isotopic invariance of the strong interactions, the ηp and ηn scattering lengths must be equal. If we do not make any distinction between the radii of the η nuclei ^{3}He and T, then their wave functions will be identical. To find the wave functions of the η meson in the nucleus we

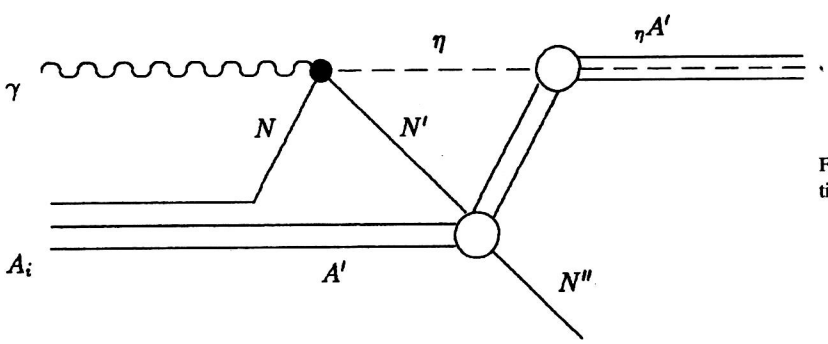

FIG. 8. Schematic diagram of the mechanism for photoproduction of η nuclei in the reaction $\gamma+A\rightarrow N+{}_{\eta}A'$.

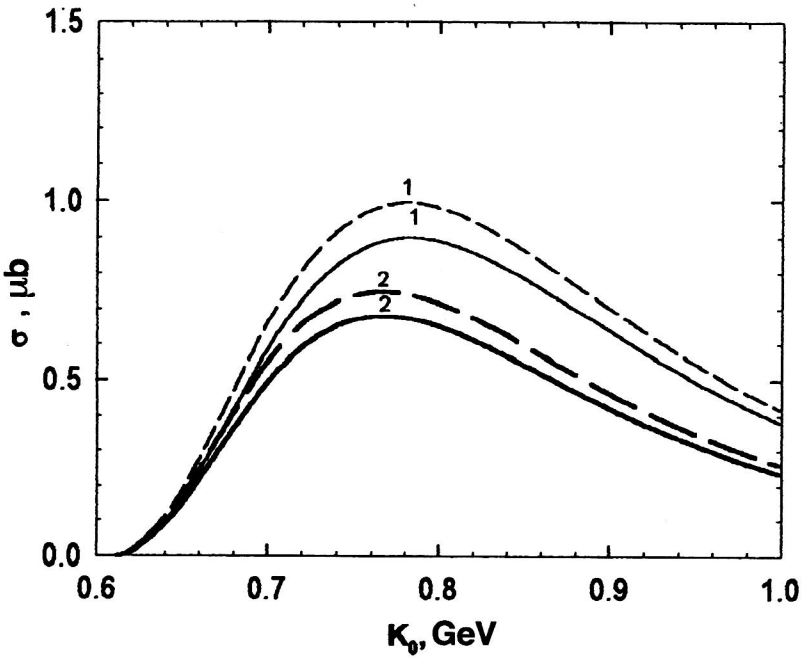

FIG. 9. Dependence of the total cross section for the reactions ^{4}He$(\gamma,p)_\eta$T (curves 1) and ^{4}He$(\gamma,n)^3_\eta$He (curves 2) on the incident γ energy, with (solid lines) and without (dashed lines) the final-state interaction of the nucleons.

use the ηN scattering lengths from recent theoretical studies.[22,23] The values of a_0 in these studies are not essentially different, and therefore in the calculations we shall use only the single value (17) from Ref. 22. Choosing the radii of superlight η nuclei to be $R_{eq}=2.45$ F, which corresponds to the rms radius $\langle r^2\rangle^{1/2}=1.9$ F, we obtain a bound state with energy eigenvalue

$$E=(2.30+i5.50)\ \text{MeV}.$$

In the simple nuclear shell model, the amplitude of the reaction (45) will have the form

$$\langle f|\hat{T}_{\eta A}|i\rangle=(-1)^{\alpha+\xi+1}\sum_S \chi^+_\alpha(S)\hat{t}^\lambda_p(S)\chi_\xi(S)\cdot G_{00}(\mathbf{Q}_f), \tag{47}$$

$$G_{00}(\mathbf{Q}_f)=f(V_R,V_I)\cdot\int d^3r e^{i\mathbf{Q}_f\mathbf{r}}\varphi_{00}(\mathbf{r})\varphi^{1s}_\eta(\mathbf{r}), \tag{48}$$

where $\mathbf{Q}_f=\mathbf{k}-\mathbf{p}_f$ is the momentum transferred to the η nucleus; $\varphi_{00}=R_{00}(r/r_0)N_0/\sqrt{4\pi}$ is the spatial part of the nucleon wave function in ^{4}He in the oscillator shell model with normalization factor N_0; $\varphi^{1s}_\eta(\mathbf{r})$ is the normalized wave function of the relative motion of the η meson and the nuclear core; and f is a factor taking into account the final-state interaction of the proton with the nucleus in the form (34) with $V_R=0$. The quantity G_{00} can be written as

$$G_{00}(\mathbf{Q}_f)=f\cdot\sqrt{\frac{16\pi}{Q_f^2r_0^3}}\int_0^\infty dr\cdot r\sin(Q_fr)e^{-r^2/2r_0^2}\varphi^{1s}_\eta(\mathbf{r})$$

$$=f\cdot\sqrt{\frac{16\pi}{Q_f^2r_0^3}}I_{0s}(Q_f). \tag{49}$$

The differential cross section for the reaction (45), averaged over the photon polarizations and summed over the polarizations of the emitted proton, will have the form

$$\frac{d\sigma}{d\Omega_p}=\frac{16\sqrt{\pi}}{Q_f^2r_0^3}K_2\sum_\lambda\left(|K^p(\lambda)|^2+|\mathbf{L}^p(\lambda)|^2\right)\cdot|I_{0s}(Q_f)|^2\cdot|f(V_I)|^2, \tag{50}$$

where the kinematical factor K_2 in the lab frame is given by

$$K_2=(2\pi)^{-2}\frac{\mathbf{P}_f^2p_{0f}Q_{0f}}{|\mathbf{P}_f|(k_0+Q_{0i})-k_0p_{0f}\cos\theta_p}. \tag{51}$$

We also obtain an expression similar to (50) for the cross section of the reaction (46), in which instead of the amplitude for meson photoproduction on the proton we have the amplitude for photoproduction on the neutron.

In Fig. 9 we show the results of the calculations of the total cross sections for the reactions (45) and (46), with and without the nucleon final-state interaction as a function of the incident γ energy. The cross sections for the two reactions reach their largest value at a photon energy $K_0=770$ MeV. The manifestation of the $S_{11}(1535)$ resonance in the nuclear cross sections is smoothed compared with the cross sections for the corresponding elementary processes, owing to the inclusion of the Fermi motion of the intranuclear nucleons according to the spectator model.[41] The final-state interaction of the protons and neutrons (for which the same nucleon–nucleus potential was used) leads to an insignificant decrease of the reaction cross sections (Fig. 9). Owing to the difference of the cross sections for η-meson photoproduction on protons and neutrons, the cross section for the reaction (45) is expected to be larger than that for (46) at the γ energies in question. The calculated widths of the η nuclei $^3_\eta$He and $_\eta$T (≈ 10 MeV) turned out to be the same as those first predicted in Refs. 3 and 4, but for η nuclei heavier than $^{16}_\eta$O. Given this sizable lifetime of superlight η nuclei, one can expect to find them in the reactions (45) and (46) on the basis of the

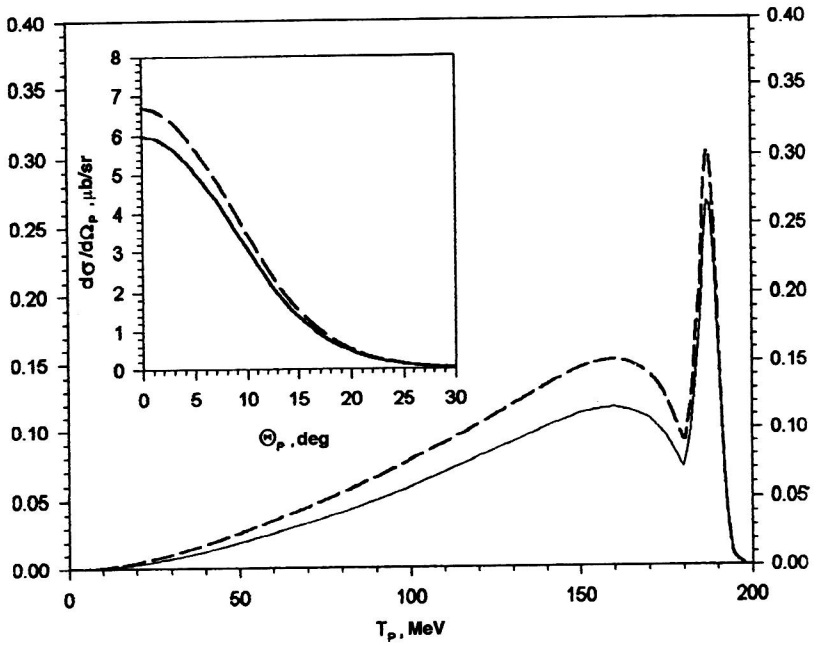

FIG. 10. Differential cross section of the reaction ^{4}He$(\gamma,\eta p)$T for photon energy $K_0=760$ MeV and proton emission angle $\theta_p=10°$ as a function of the proton energy in the lab frame. The solid lines (dashed lines) show the result of the calculations with (without) the proton interaction in the final state. The peak shows the differential cross section of the reaction ^{4}He$(\gamma,p)_\eta$T for the given kinematical conditions, smeared over the width of the η-nucleus level according to a normal distribution. The inset shows the dependence of the differential cross section for the reaction ^{4}He$(\gamma,p)_\eta$T on the proton emission angle at photon energy $K_0=760$ MeV.

peak in the spectrum of emitted nucleons from inclusive ^{4}He(γ,N) reactions. The differential cross sections for the reactions

$$\gamma+{}^4\mathrm{He}\rightarrow p+\eta+T, \tag{52}$$

$$\gamma+{}^4\mathrm{He}\rightarrow n+\eta+{}^3\mathrm{He}, \tag{53}$$

of photoproduction of slow but unbound η mesons will vary most strongly with the nucleon energy (at fixed photon energy). It is therefore important to know the angular and energy distributions of the particles in such reactions. Let us discuss the reaction (45) in more detail as a candidate for finding light η nuclei.

The differential cross section for the reaction (45) calculated for γ energy $K_0=760$ MeV is shown as a function of the proton emission angle in the inset of Fig. 10. The dependence of the doubly differential cross section for the reaction (52) on the energy of the ejected proton for emission angle $\theta_p=10°$ and the same photon energy is shown. The differential cross section for the reaction (45) is taken at proton emission angle $\theta_p=10°$ in the lab frame and smeared over the width of the level of the η nucleus $_\eta$T according to a normal distribution, which is also shown.

The results of the calculation inspire hope. The estimated signal-to-background ratio depends on the proton emission angle and for $\theta_p=5°$, 10°, and 15° is respectively 3.7/1, 2.9/1, and 2/1 (Fig. 10). More refined calculations may change this ratio in one direction or the other, but not drastically. The width of the gap between the quasielastic peak of ejected protons in the reaction (52) and the peak corresponding to protons from the reaction (45) is determined by the binding energy and width of the level of the η nucleus $_\eta$T (see Fig. 10). The uniqueness of the η nuclei $^3_\eta$He and $_\eta$T should be noted. It is they (and perhaps $_\eta$D) which can have such small level widths and binding energies, owing to their small density. The next heaviest η nucleus $^4_\eta$He will have energy eigenvalue

$$E=(17.5+i16.9)\ \mathrm{MeV},$$

for the ηN scattering length (17), decreasing the signal-to-background ratio in the corresponding $^4_\eta$He photoproduction reaction by more than a factor of three in relation to $^3_\eta$He production.

The identification of η nuclei in the reaction (45) requires tagged photons of high intensity with energy resolution of at least 2–3 MeV. Since the reaction (45) is a two-particle reaction, there is a strong connection between the energy and angle of the emitted nucleon, and so if a peak is observed in the expected place in the spectrum of nucleons from the inclusive photoreaction

$$\gamma+{}^4\mathrm{He}\rightarrow p+\cdots, \tag{54}$$

this would indicate the production of η nuclei in the reaction (45). The height and width of the peak are proportional to the cross section for the reaction (45) [if neutrons are recorded, then to the cross section for the reaction (46)], and the width is proportional to the width of the η-nucleus level.

The calculations of the inclusive cross section for the reaction (54) at $K_0\approx 800$ MeV, like those of the absolute background for the reaction (45), are complicated. We only note that the inclusive cross section will be the sum of the cross sections for two-, three-, and four-particle photodisintegration of the ^{4}He nucleus, the cross sections for single and double pion photoproduction, and, finally, the cross sections for the studied reaction (52).

3.3. Photoproduction of η nuclei in 1s states

In contrast to the photoproduction of superlight η nuclei with number of nucleons $A<4$, η nuclei with $A>6$ can be produced not only in the 1s state (see Table I). In addition, for nuclei with $A>6$ it is necessary to take into account the low-lying excited states of the nucleon cores themselves, the excitation of which (if their widths are less than 1 MeV) will

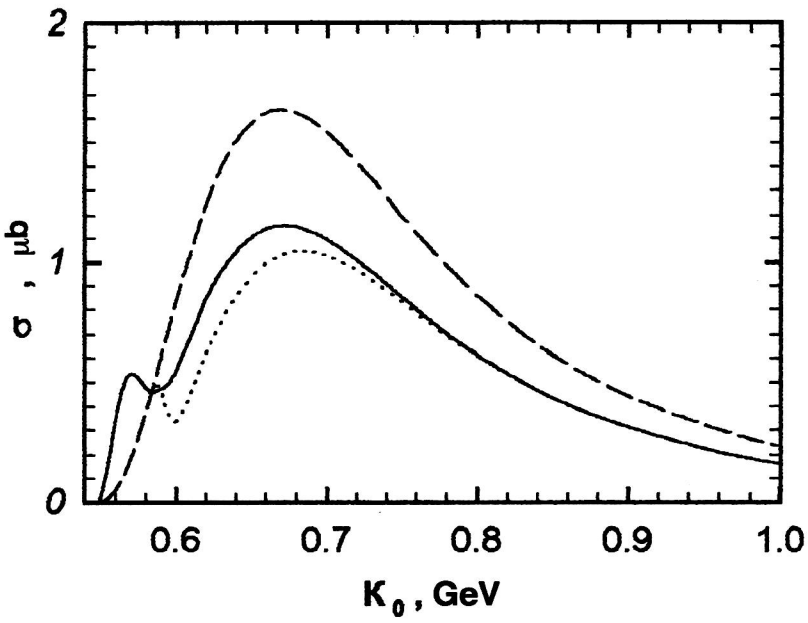

FIG. 11. Dependence of the total cross section for the reaction $^{12}C(\gamma,p)^{11}_{\eta}B_{g.s.}$ on the incident γ energy, neglecting the final-state interaction (dashed line) and including it, both with the full nuclear optical potential (dotted line) and without the real part (solid line). The proton interaction near the reaction threshold in the two cases was taken into account according to the results of Ref. 56, using the method suggested in Ref. 57.

be assumed to have no effect on the production and existence of η nuclei. In this connection it should be noted that nucleon knockout from the s shells of nuclei with $A>5$ leads to highly excited nuclear states of the particle–hole type, whose lifetimes are of the same order as those of η nuclei. The properties of η nuclei with nucleon cores in highly excited states will also be determined by the instability of the nucleon core, and therefore they require special study beyond what we undertake here. We shall consider the reaction (4) on ^{12}C and ^{16}O nuclei leading to the production of η nuclei in the $1s$ state.

Using the approximations that we have discussed, we write down the amplitude of the reaction (4) on p-shell nuclei ($4<A<16$) by analogy with the amplitude for η-meson photoproduction on nuclei with nucleon knockout [see Eqs. (24)–(26)]:

$$\langle f|\hat{T}^{1s}_{\eta A}|i\rangle=\sqrt{A-4}\langle\psi_f|\varphi^{*1s}_{\eta}(\mathbf{r}_1)\cdot f\cdot e^{i(\mathbf{k}-\mathbf{p}_f)\mathbf{r}_1}t^{\lambda}_1(S_1,t_1)\cdot\varepsilon_{\lambda}|\psi_i\rangle$$
$$=\sqrt{\frac{A-4}{12}}\sum_{m,\xi}(-1)^{\xi-J_f+m}\times\langle 1m,\tfrac{1}{2}\xi|J_f-M_f\rangle H^{\alpha\beta}_{\xi r}(\lambda)G^0_{1m}(Q_f), \quad (55)$$

where

$$G^0_{1m}(Q_f)=f\cdot\int d^3r_1 e^{iQ_f r_1}\varphi_{1m}(\mathbf{r}_1)\varphi^{*1s}_{\eta}(\mathbf{r}_1)$$
$$=f\cdot i4\pi N_1 Y'_m(\mathbf{Q}_f)\frac{1}{Q_f^2}\cdot I_{0p}(Q_f), \quad (56)$$

$$N_1=\left[\frac{8}{3r_0^5\sqrt{\pi}}\right]^{1/2}, \quad (57)$$

$$I_{0p}(Q_f)=\int dr_1 r_1[\sin(Q_f r_1)-Q_f r_1\cos(Q_f r_1)]\varphi^{*1s}_{\eta}\times(\mathbf{r}_1)e^{-r_1^2/2r_0^2}, \quad (58)$$

and φ^{1s}_{η} is the η-meson wave function in the nucleus.

The differential cross sections for the reactions

$$\gamma+{}^{12}C\rightarrow p+\eta^{11}E_{g.s.}(1s), \quad (59)$$

$$\gamma+{}^{16}O\rightarrow p+\eta^{15}N_{g.s.}(1s), \quad (60)$$

when the nucleon cores of the produced η nuclei $^{11}_{\eta}B$ and $^{15}_{\eta}N$ are in the ground state, can be written as

$$\frac{d\sigma}{d\Omega_p}=K_2\frac{z\sqrt{\pi}}{Q_f^4 r_0^5}\sum_{\lambda}(|K^p(\lambda)|^2+|\mathbf{L}^p(\lambda)|^2)\cdot|I_{0p}(Q_f)|^2|f|^2, \quad (61)$$

where for the reaction (59)

$z=128/9$,

and for (60)

$z=32/3$.

Since the expressions for the cross sections of the reactions (59) and (60) differ only by a constant, it is sufficient to study only one of them. In Fig. 11 we show the total cross section for $^{11}_{\eta}B(1s)$ production in the reaction (59) as a function of the photon energy, with and without the final-state interaction. The thresholds of the reactions (4) are determined by the mass of the produced η nuclei. The calculated threshold of the reaction (59) is nearly 60 MeV lower than the thresholds of (45) and (46); accordingly, its cross section reaches a maximum at $K_0\approx 670$ MeV. In order to estimate how the results of our calculations depend on the parameters of the model for the η nucleus, in Fig. 12 we show the dependence of the total cross section for the reaction (59) on the radius of the η-nucleus optical potential. For the extreme values $r_0=1.2$ F and $r_0=1.5$ F the deviation from the above

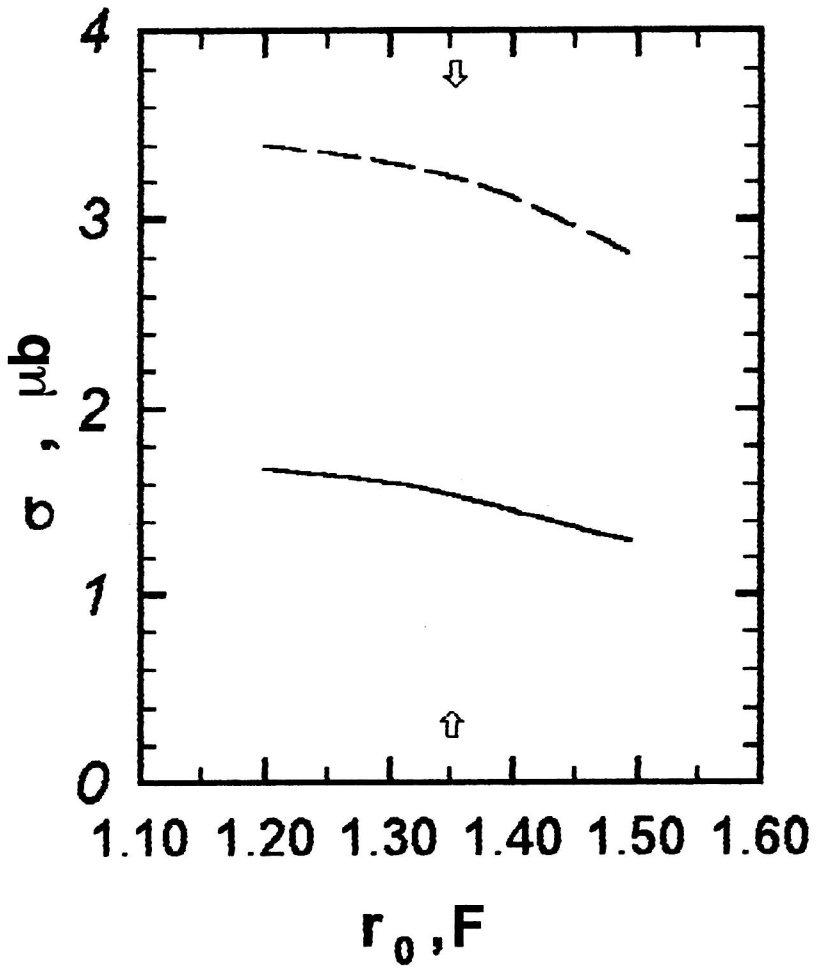

FIG. 12. Dependence of the total cross sections for the reactions $^{12}C(\gamma,p)^{11}_{\eta}B_{g.s.}(1s)$ (solid line) and $^{12}C(\gamma,p)^{11}_{\eta}B^*(1p)$ (dashed line) on the radius $r_0 = R_{eq}A^{-1/3}$ of the η nucleus at the γ energy $K_0 = 700$ MeV. The arrow indicates the value of r_0 used in these calculations.

result is $+9\%$ and -17%, respectively. Another important parameter of the model is the ηN scattering length. In Fig. 13 we show the total cross section for the reaction (60) as a function of the photon energy for various depths of the η-nucleus square-well potential (5), obtained by using different values of a_0 (Refs. 21–23). An insignificant change of the cross section is observed only in the near-threshold region of γ energies.

To demonstrate the possible effect of the final-state interaction near threshold, we considered a model which de-

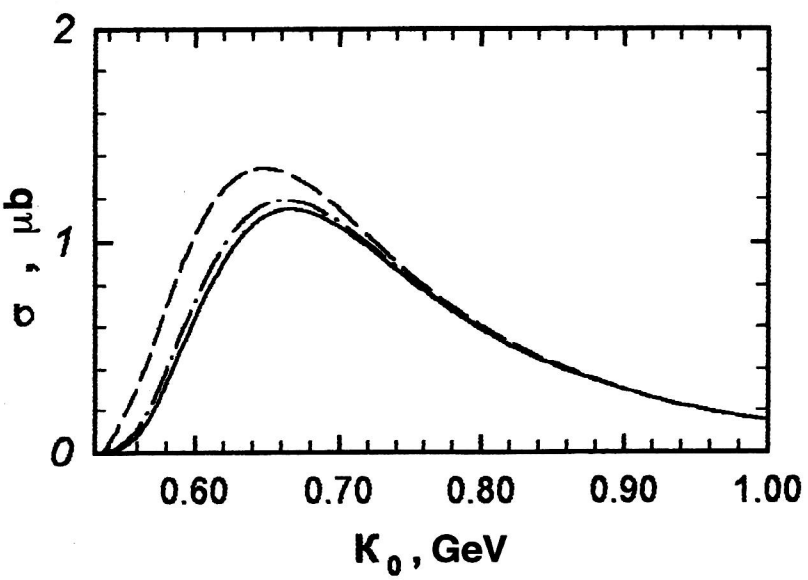

FIG. 13. Dependence of the total cross section for the reaction $^{16}O(\gamma,p)^{15}_{\eta}N_{g.s.}(1s)$ on the incident γ energy for the following values of the ηN scattering length in the η-nucleus potential (5): $a_0 = (0.880 + i0.274)$ F (Ref. 21; dashed line); $a_0 = (0.717 + i0.263)$ F (Ref. 22; solid line); $a_0 = (0.751 + i0.274)$ F (Ref. 23; dot–dash line).

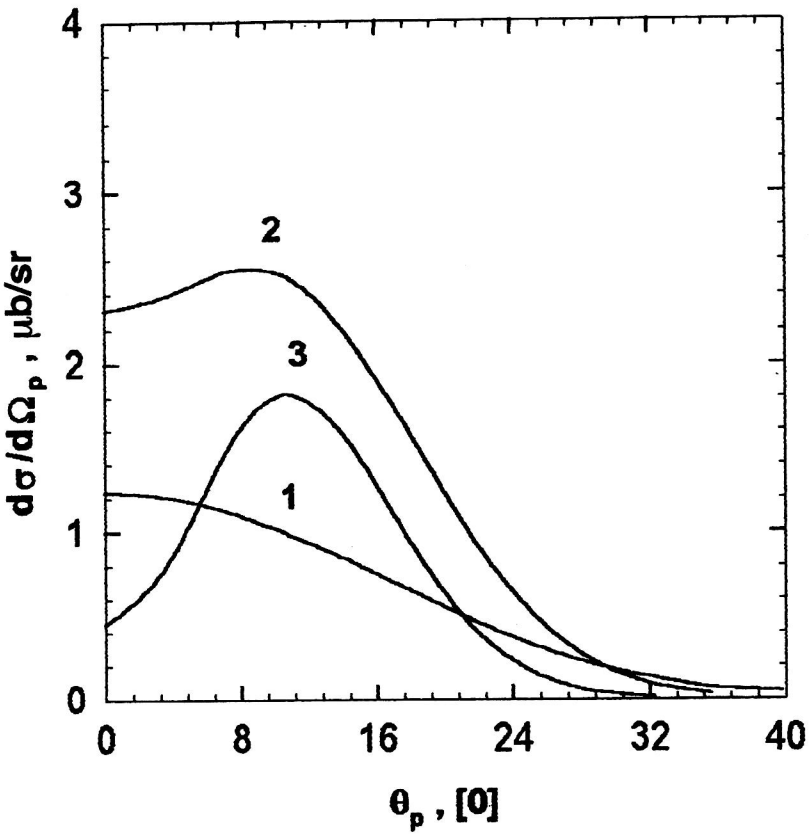

FIG. 14. Proton angular distribution for the reaction $^{12}C(\gamma,p)^{11}_{\eta}B_{g.s.}$ in the lab frame at various incident γ energies: $K_0=600$ MeV (curve 1); $K_0=700$ MeV (curve 2); $K_0=800$ MeV (curve 3). The nuclear optical potential without the real part was used to include the final-state interaction.

scribes the nucleon interaction at $T_p<40$ MeV where, as is well known, nucleons interact with nuclei via the giant dipole resonance. Using the results of Ref. 56, we reconstructed the effect of this interaction for the reaction (59) according to the method of Ref. 57 up to the emitted-γ energy $K_0=580$ MeV (Fig. 11). We note that this result should be viewed as qualitative, namely, as what can be expected from the final-state interaction at threshold for reactions like (4). Beginning at proton energies $T_p>50$ MeV, the inclusion of the final-state interaction for the reaction (59) leads only to a decrease of its cross section. The inclusion of the full nuclear optical potential in this model leads to a larger suppression of the cross section than the inclusion of only the imaginary part up to the emitted-proton energy 300 MeV. At higher nucleon energies the real part of the optical potential can be neglected (see Fig. 11). The angular distribution of protons from the reaction (59) is shown in Fig. 14. It has a typical forward directionality. As the energy of the incident photon increases, a maximum appears in the angular distribution at $\theta_p\approx 12°$. It does not occur in the angular distributions of the reactions (45) and (46), and its location is stable with respect to variations of the photon energy in this range (Fig. 14).

The differential cross section for the reaction

$$\gamma+{}^{12}\mathrm{C}\rightarrow p+{}^{11}_{\eta}B^{*}(1s), \tag{62}$$

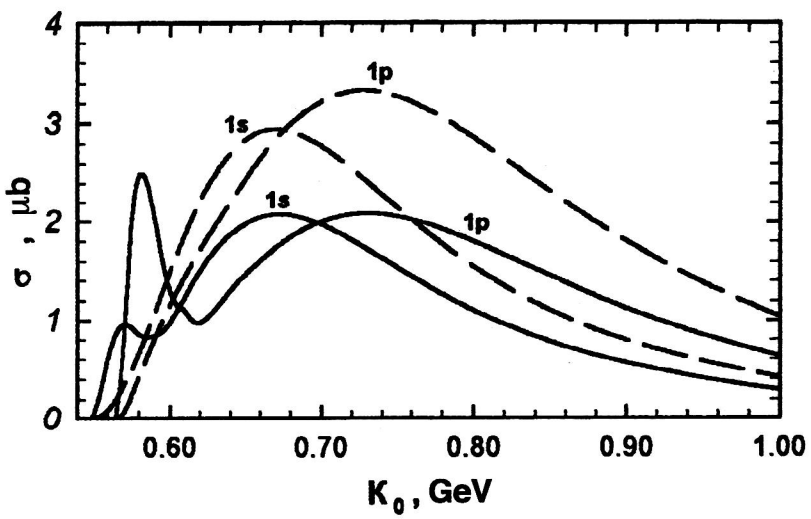

FIG. 15. Total cross sections for the reactions $\gamma+{}^{12}\mathrm{C}\rightarrow p+{}^{11}_{\eta}\mathrm{B}^{*}(1s)$ and $\gamma+{}^{12}\mathrm{C}\rightarrow p+{}^{11}_{\eta}\mathrm{B}^{*}(1p)$ as functions of the incident γ energy, calculated with (solid lines) and without (dashed lines) the final-state interaction.

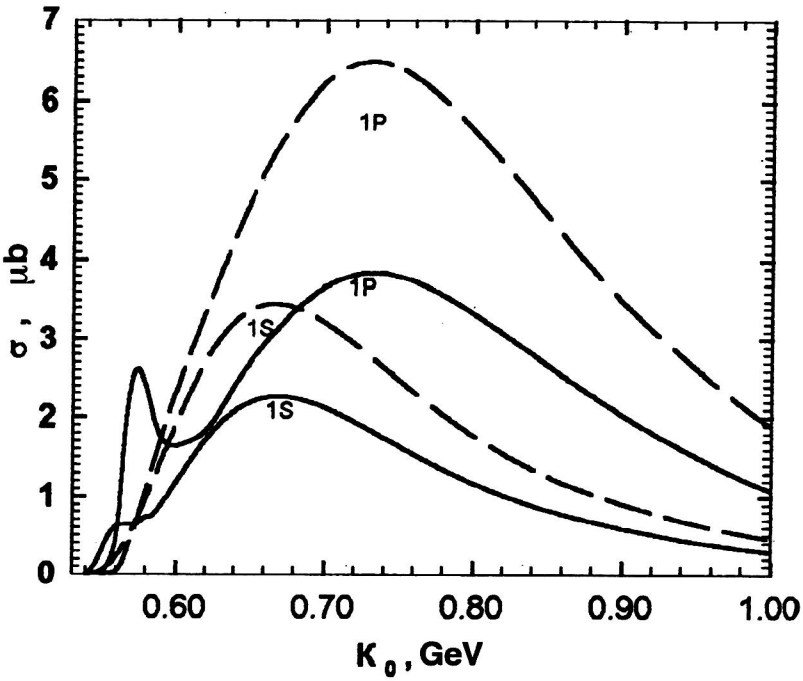

FIG. 16. The same as in Fig. 15, for the target nucleus ^{16}O.

where the η nucleus is formed with a nucleon core in the ground state (35) or in an excited state (35a) or (35b), can be written as

$$\frac{d\sigma}{d\Omega_p}=K_2\frac{z\sqrt{\pi}}{Q_f^4 r_0^5}\sum_{\lambda}\left(|K^p(\lambda)|^2+|\mathbf{L}^p(\lambda)|^2\right)\cdot|I_{0p}(Q_f)|^2|f|^2, \tag{63}$$

with

$$z=(192+128\,\alpha)/9.$$

Similarly, the differential cross section of the reaction

$$\gamma+{}^{16}\mathrm{O}\rightarrow p+{}^{15}_{\eta}\mathrm{N}^*(1s), \tag{64}$$

when the nucleon core $^{15}_{\eta}$N remains in the ground state or the first excited state, reduces to Eq. (63) with

$$z=32.$$

The total cross sections of the reactions (62) and (64) are shown in Figs. 15 and 16 as functions of the incident γ energy. The cross sections for these reactions are two to three times larger than the corresponding cross sections for the reactions (59) and (60), in which the nuclear cores remain only in the ground state. Neither the proton energy nor the angular distribution, which has the form shown in Fig. 14, appears to allow the isolation of photoproduction of η nuclei with different excited states of the nucleon core, and therefore we shall consider all such reactions together. We note that the energy distribution of protons from the reactions (62) and (64) will be smeared not only over the large widths of the produced η nuclei $^{11}_{\eta}$B$(1s)$ and $^{15}_{\eta}$N$(1s)$, but also over the excitation energies of their nucleon cores. Therefore, the method of detecting η nuclei by isolating peaks in the proton (neutron) energy spectrum of the reaction (4) with nuclei heavier than ^{4}He will be less effective than in the reactions (45) and (46). In connection with this it is interesting to detect η nuclei from their correlated decay products (see Ref. 58) together with "fast" nucleons from the reaction (4).

3.4. Photoproduction of η nuclei in the $1p$ state

An η nucleus with more than six nucleons can be produced in the capture of an η meson into the $1s$ or $1p$ orbit (Table I). The photoproduction of η nuclei in the $1p$ state will differ from ${}_{\eta}A(1s)$ production in reactions like (4), and it therefore requires special study. In order to reduce the awkward angular-momentum algebra to a minimum, we shall study reactions of the form

$$\gamma+A_i\rightarrow N+{}_{\eta}A'(1p) \tag{65}$$

on nuclei with quantum numbers equal to zero, such as ^{12}C and ^{16}O. We write the amplitudes of these reactions by analogy with those of $(\gamma,\eta N)$ reactions on the same nuclei [see Eq. (30)]:

$$\langle f|\hat{T}^{1p}_{\eta A}|i\rangle=\sqrt{\frac{A-4}{12}}\sum_{m,\xi,\nu}(-1)^{\xi+m}\langle 1-m,1\nu|l\nu-m\rangle$$
$$\times\langle l\nu-m,1/2-\xi|J_fM_f\rangle H^{\alpha\tau}_{\xi\tau}(\lambda)G^{1\nu}_{lm}(\mathbf{Q}_f). \tag{66}$$

In the angular-momentum representation $G^{1\nu}_{1m}$ is

$$G^{1\nu}_{1m}(\mathbf{Q}_f)=4\pi N_l N_\eta\sum_{\aleph=0}^{\infty}\sum_{n=-\aleph}^{\aleph}(i)^{\aleph}Y^{\aleph}_n(\mathbf{G}_f)$$
$$\times\int_{\Omega_r}\int[Y^{\aleph}_n(\mathbf{r})]^*Y^1_m(\mathbf{r})Y^1_\nu(\mathbf{r})d\Omega_r$$
$$\times\int_0^\infty j_{\aleph}(Q_f r)re^{r^2/2r_0^2}\frac{u_l(r)}{r}r^2d. \tag{67}$$

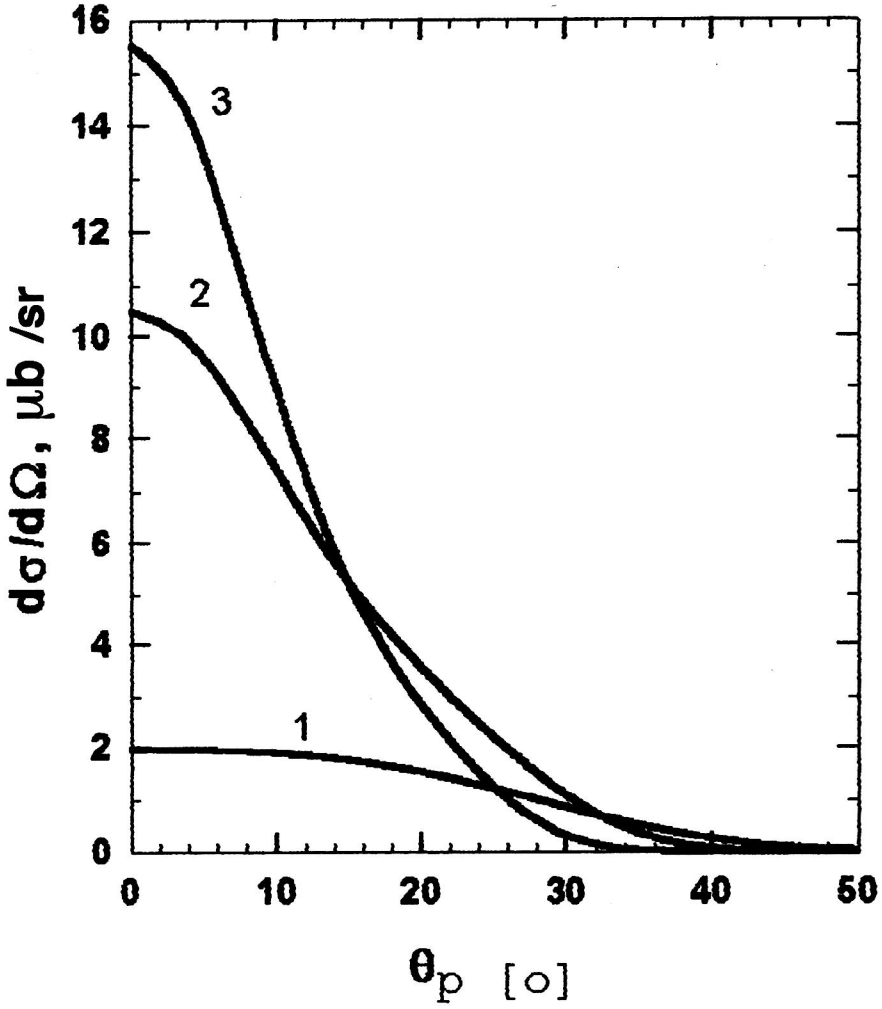

FIG. 17. Angular distribution of protons from the reaction $^{16}O(\gamma,p)^{15}_{\eta}N^*(1p)$ in the lab frame for the photon energies $K_0=600$ MeV (curve 1), $K_0=700$ MeV (curve 2), and $K_0=800$ MeV (curve 3), calculated with allowance for the final-state interaction.

Using the standard algebra of the spherical harmonics, $G^{1\nu}_{1m}$ can be brought to the form

$$G^{1\nu}_{1m}(\mathbf{Q}_f)=N_l N_\eta\left[I_{10}(Q_f)-\sqrt{\frac{24\pi}{5}}Y^2_{m+\upsilon}(\mathbf{r})\right.$$
$$\left.\times\langle 1m,1\nu|2m+\nu\rangle I_{12}(Q_f)\right]. \quad (68)$$

In addition to that used earlier, in (67) we have introduced some new notation. We use the dimensional quantity

$$I_{1\aleph}(Q_f)=\int_0^\infty j_\aleph(Q_f r)e^{r^2/2r_0^2}u_1(r)r^2 d, \quad (69)$$

where $j_\aleph(z)$ is the spherical Bessel function, and $u_\ell(r)$ is the solution of Eq. (12) and is the radial part of the radial wave function of the η nucleus in the $1p$ state,

$$\varphi^{1\upsilon}_\eta(\mathbf{r})=N_\eta\frac{u_l(r)}{r}\cdot Y^1_\upsilon(\mathbf{r}), \quad (70)$$

normalized to unity by the normalization factor N_η. Let us consider the production of $1p$ η nuclei with nucleon cores in all possible excited states:

$$\gamma+{}^{12}C\to p+{}^{11}_{\eta}B^*(1p), \quad (71)$$

$$\gamma+{}^{16}O\to p+{}^{15}_{\eta}N^*(1p). \quad (72)$$

This makes it possible to use the completeness of the spin states for calculating the squared moduli of their amplitudes (66). Using rather awkward angular-momentum algebra, the differential cross sections for the reactions (71) and (72) can be written as a single expression:

$$\frac{d\sigma}{d\Omega_p}=z\cdot K_2\frac{|N_\eta|^2}{r_0^5\sqrt{\pi}}\sum_\lambda(|K^P(\lambda)|^2+|\mathbf{L}^P(\lambda)|^2)\left\{5|I_{10}(Q_f)|^2\right.$$
$$+[\sqrt{2}(9\cos^2\theta-5)-6\cos^2\theta-2]\mathrm{Re}[I_{10}(Q_f)$$
$$\left.\cdot I^*_{12}(Q_f)]+\frac{26+2\sqrt{2}(5-9\cos^2\theta)}{3}\cdot|I_{12}(Q_f)|^2\right\}, \quad (73)$$

where θ is the emission angle of the produced η nucleus. For the reaction (71)

$$Z=16/9,$$

and for (72)

$$Z=8/3.$$

In Figs. 15 and 16, along with the cross sections for the

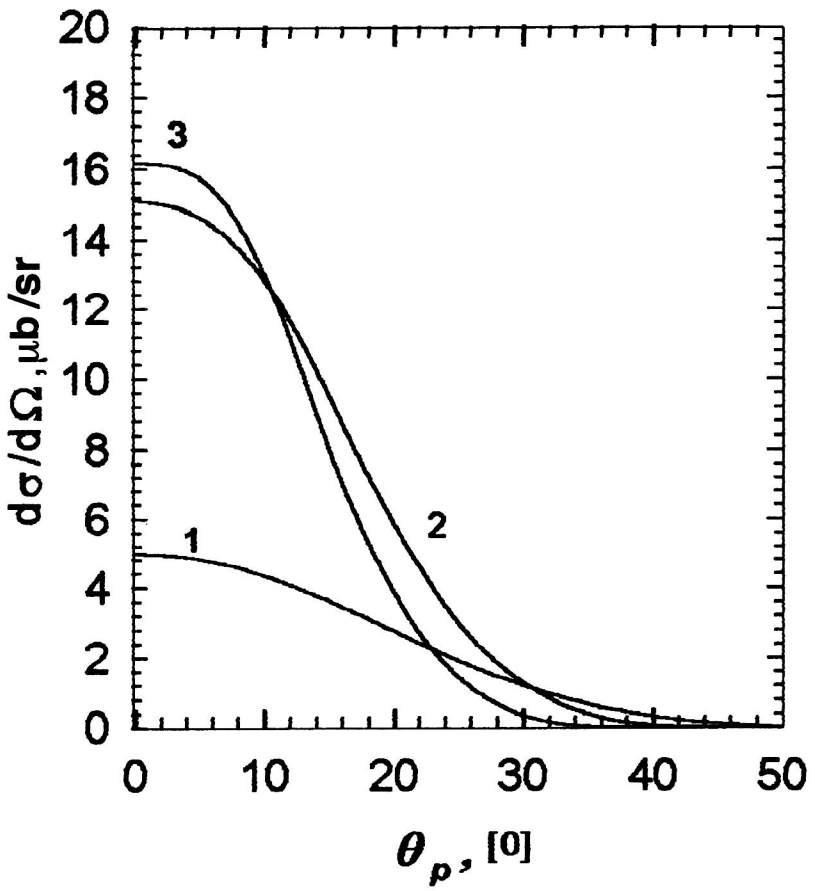

FIG. 18. Summed angular distribution of protons from the reaction $^{16}O(\gamma,p)^{15}_{\eta}N^*$ for production of the η nucleus $^{15}_{\eta}N^*$ in the $1s$ and $1p$ states. The other notation is the same as in Fig. 17.

reactions (62) and (64), we show the results of calculating the total cross sections for the reactions (71) and (72). We see that the cross sections for η-nucleus production in the $1p$ state are much larger than those for photoproduction of the corresponding η nuclei in the $1s$ state. One reason for this is the different volumes of phase space of the final particles, which for the reactions (65) is larger than for the corresponding reactions

$$\gamma+A_i\rightarrow N+{}_{\eta}A'(1s). \tag{74}$$

Another feature of the production of $1p-\eta$ nuclei by photons is the shift of the broad maxima in their cross sections toward higher energies ($\approx$80 MeV) relative to the maxima in the cross sections for the reactions (74) (Figs. 15 and 16). The high rate of growth of the cross section from threshold for η-nucleus production in the $1p$ state in com-

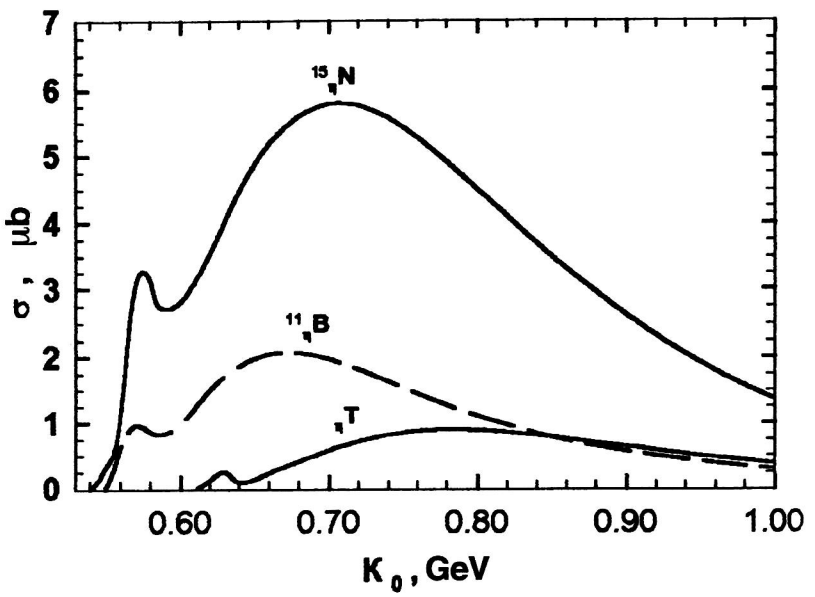

FIG. 19. Dependence of the total cross sections of the reactions $^4He(\gamma,p)_{\eta}T$, $^{12}C(\gamma,p)^{11}_{\eta}B^*(1L)$, and $^{16}O(\gamma,p)^{15}_{\eta}N^*(1L)$ on the incident γ energy, taking into account the final-state interaction.

parison with the $1s$ state can lead to high, narrow peaks in the cross sections for $A(\gamma,N)_{\eta}A'(1p)$ reactions near threshold, owing to the final-state interaction (see the $1p$ curves in Figs. 15 and 16).

The differential cross section for the reaction (72) at various incident γ energies is shown in Fig. 17. The forward directivity of the nucleon emission, which is even larger than in the case of η-nucleus production in the $1s$ state, should be noted. The cross sections are largest at $\theta_p=0°$ and decrease sharply with increasing angle (Fig. 17). The most important problem at present is the experimental confirmation of the existence of η nuclei with $A>6$, and therefore it is essential to know the cross section for their production in all possible states. This cross section will be the sum of those for η-nucleus photoproduction in the $1s$ and $1p$ states, owing to the orthogonality of the wave functions of these states of η nuclei. The proton angular distribution for $^{15}_{\eta}$N production in all possible states is shown in Fig. 18 for various incident γ energies. Although the differential cross section is again largest at zero angle, it begins to decrease strongly with increasing proton emission angle only after passing through $\theta_p \approx 12°$. The cross sections in the angular range $\theta_p \approx 0-12°$ are large. Finally, the total cross sections for production of the η nuclei $_{\eta}$T, $^{11}_{\eta}$B*, and $^{15}_{\eta}$N* in all possible states for different nucleon cores and excitation levels are given as functions of the photon energy in Fig. 19. Although the cross sections for η-nucleus photoproduction increase rapidly with increasing atomic number of the target nuclei, the widths of the produced η nuclei also increase strongly with increasing A, making it difficult to detect η nuclei with the number of nucleons $A>12$.

CONCLUSION

The present complicated situation regarding η nuclei involves many contradictions: η nuclei appear just where they are not expected! The heavy η nuclei with $A>12$ predicted in early studies apparently have properties very different from those suggested earlier in Refs. 3 and 4, and this has made their experimental discovery difficult. In addition, for decades we have been living in the shadow of the anomaly in the cross sections for η-meson production near threshold in few-nucleon systems, and dozens of theoreticians have tried to explain the increase of the interaction strength in η-meson–nucleus systems with decreasing energy. However, all these early attempts have been clumsy and did not resort to the hypothesis that superlight η nuclei exist. The prediction of the properties of η nuclei with $A>6$ and their discovery on the basis of these properties will apparently give a definitive answer to the question of the existence of η nuclei, and then they can be studied systematically. Otherwise, it will be necessary to answer the more difficult question of why η nuclei do not exist.

I would like to thank A. I. Lebedev for suggesting this research, A. I. L'vov, G. M. Radutskiĭ, and A. I. Fiks for fruitful discussions, A. V. Kolchin for a helpful remark, and Yu. F. Krechetov for supporting this study.

[1] Particle Data Group, Phys. Rev. D **50**, 1173 (1994).
[2] V. V. Baru and A. E. Kudryavtsev, Yad. Fiz. **60**, 1620 (1997) [Phys. At. Nucl. **60**, 1475 (1997)].
[3] L. C. Liu and Q. Haider, Phys. Lett. B **172**, 257 (1986); **174**, 465(E) (1986).
[4] L. C. Liu and Q. Haider, Phys. Rev. C **34**, 1845 (1986).
[5] R. E. Crien, S. Bart, P. Pile *et al.*, Phys. Rev. Lett. **60**, 2595 (1988).
[6] R. E. Crien, Czech. J. Phys., Sect. B **39**, 914 (1989).
[7] H. C. Chiang, E. Oset, and L. C. Lui, Phys. Rev. C **44**, 738 (1991).
[8] J. D. Johnson, G. R. Burleson, C. Edwards *et al.*, Phys. Rev. C **47**, 2571 (1993).
[9] R. Frascaria, F. Roudot, R. Wurzinger *et al.*, Phys. Rev. C **50**, R537 (1994).
[10] P. Berthet *et al.*, Nucl. Phys. A **443**, 589 (1985).
[11] L. C. Liu, Preprint LA-UR-94-2338, Los Alamos National Laboratory, Los Alamos (1994).
[12] N. Willis, Y. Le Bornec, A. Zghiche *et al.*, Preprint IPNO-DRE-97-09 (1997).
[13] B. Krusche, J. Ahrens, G. Anton *et al.*, Phys. Rev. Lett. **74**, 3736 (1995).
[14] B. Krusche, in *Proceedings of the Twenty-Third Intern. Workshop on the Gross Properties of Nuclei and Nuclear Excitation*, GSI, Darmstadt (1995).
[15] T. E. O. Ericson and W. Weise, *Pions and Nuclei* (Clarendon Press, Oxford, 1988) [Russ. transl., Nauka, Moscow, 1991].
[16] L. R. B. Elton, *Nuclear Sizes* (Oxford University Press, London, 1961) [Russ. transl., IL, Moscow, 1962].
[17] R. S. Bhalero and L. C. Liu, Phys. Rev. Lett. **54**, 865 (1985).
[18] M. Arima, K. Shimizu, and K. Yazaki, Nucl. Phys. A **543**, 619 (1992).
[19] C. Wilkin, Phys. Rev. C **47**, R938 (1993).
[20] V. V. Abaev and B. M. K. Nefkens, Preprint UCLA-10-P25-229, University of California, Los Angeles (1994).
[21] M. Batinic and A. Svarc, Preprint IRB-FEP-03/95, Rudjuer Boskovic Institute, Zagreb (1995).
[22] M. Batinic, I. Dadic, I. Slaus *et al.*, Preprint IRB-FEP-02-96, Rudjuer Boskovic Institute, Zagreb (1996).
[23] A. M. Green and S. Wycech, Preprint HIP-1997-08 (1997).
[24] R. L. Anderson and R. Prepost, Phys. Rev. Lett. **23**, 46 (1969).
[25] R. Bilger *et al.*, in *Proceedings of the Fourteenth Intern. Conf. on Particles and Nuclei*, edited by C. E. Carlson and J. J. Domingo (World Scientific, Singapore 1996), p. 401.
[26] L. A. Kondratyuk, A. V. Lado, and Yu. N. Uzikov, Yad. Fiz. **58**, 524 (1995) [Phys. At. Nucl. **58**, 473 (1995)].
[27] T. Ueda, Phys. Rev. Lett. **66**, 297 (1991).
[28] A. I. Lebedev and G. A. Sokol, Preprint No. 34, Lebedev Institute, Moscow (1995) [in Russian].
[29] A. Svarc, M. Batinic, and I. Slaus, Few-Body Syst., Suppl. **9**, 203 (1995).
[30] V. B. Belyaev, S. A. Rakityansky, S. A. Sofianos *et al.*, Few-Body Syst., Suppl. **8**, 309 (1995).
[31] S. A. Rakityansky, S. A. Sofianos, V. B. Belyaev *et al.*, Few-Body Syst., Suppl. **9**, 227 (1995).
[32] J. A. Niskanen, S. Wycech, and A. M. Green, Few-Body Syst., Suppl. **9**, 404 (1995).
[33] C. Bucci, G. Penso, G. Salvini *et al.*, Nuovo Cimento A **45**, 983 (1966).
[34] B. Delcourt, J. Lefrancois, J. P. Perez-Y-Jorba *et al.*, Phys. Lett. B **29**, 75 (1969).
[35] M. Wilhelm, Dissertation, Bonn University (1993).
[36] H. R. Hicks, S. R. Deans, D. T. Jacobs *et al.*, Phys. Rev. D **7**, 2614 (1973).
[37] M. Benmerrouche and C. Mukhopadhyay, Phys. Rev. Lett. **67**, 1070 (1991).
[38] C. Bennhold and H. Tanabe, Nucl. Phys. A **530**, 625 (1991).
[39] L. Tiator, C. Bennhold, and S. S. Kamalov, Nucl. Phys. A **580**, 455 (1994).
[40] A. Fix and H. Arenhovel, Nucl. Phys. A **620**, 457 (1997).
[41] J. M. Laget, Nucl. Phys. A **194**, 81 (1972).
[42] I. V. Glavanakov, Yad. Fiz. **49**, 91 (1989) [Sov. J. Nucl. Phys. **49**, 58 (1989)].
[43] P. S. Anan'in and I. V. Glavanakov, Yad. Fiz. **52**, 323 (1990) [Sov. J. Nucl. Phys. **52**, 205 (1990)].
[44] S. Cohen and D. Kurath, Nucl. Phys. **73**, 1 (1965).
[45] A. N. Boyarkina, *Structure of p-Shell Nuclei* [in Russian] (Moscow State University Press, Moscow, 1973).

[46] V. G. Neudachin and Yu. F. Smirnov, *Nucleon Associations in Light Nuclei* [in Russian] (Nauka, Moscow, 1969).
[47] S. Fernbach, R. Serber, and T. B. Taylor, Phys. Rev. **75**, 1352 (1949).
[48] F. X. Lee, L. E. Wright, C. Bennhold, and L. Tiator, Nucl. Phys. A **603**, 345 (1996).
[49] M. Hedayati-Poor and H. S. Sherif, Phys. Rev. C **56**, 1557 (1997).
[50] V. A. Tryasuchev, Yad. Fiz. **37**, 75 (1983) [Sov. J. Nucl. Phys. **37**, 40 (1983)].
[51] L. Chen and H.-C. Chiang, Phys. Lett. B **329**, 424 (1994).
[52] R. C. Carrasco, Phys. Rev. C **48**, 2338 (1993).
[53] A. I. Lebedev and V. A. Tryasuchev, J. Phys. G **17**, 1197 (1991).
[54] A. I. Lebedev and V. A. Tryasuchev, Yad. Fiz. **58**, 642 (1995) [Phys. At. Nucl. **58**, 586 (1995)].
[55] M. L. Goldberger and K. M. Watson, *Collision Theory* (Wiley, New York, 1964) [Russ. transl., Mir, Moscow, 1967].
[56] V. A. Zolenko and S. A. Soldatov, Yad. Fiz. **60**, 1971 (1997) [Phys. At. Nucl. **60**, 1803 (1997)].
[57] D. J. S. Findlay and R. O. Owens, Nucl. Phys. A **292**, 53 (1977).
[58] G. A. Sokol and V. A. Tryasuchev, Kratk. Soobshch. Fiz. **4**, 23 (1991) [in Russian].

Translated by Patricia A. Millard